16

PNL-2944
UC-35

Characterization of Airborne Uranium From Test Firings of XM774 Ammunition

J. A. Glissmeyer
J. Mishima

November 1979

Prepared for the U.S. Army
under U.S. Department of Energy
Contract EY-76-C-06-1830

Pacific Northwest Laboratory
Operated for the U.S. Department of Energy
by Battelle Memorial Institute

Battelle

PNL-2944

NOTICE

PACIFIC NORTHWEST LABORATORY
operated by
BATTELLE
for the
UNITED STATES DEPARTMENT OF ENERGY
Under Contract EY-76-C-06-1830

Printed in the United States of America
Available from
National Technical Information Service
United States Department of Commerce
5285 Port Royal Road
Springfield, Virginia 22151

Price: Printed Copy $____*; Microfiche $3.00

*Pages	NTIS Selling Price
001-025	$4.00
026-050	$4.50
051-075	$5.25
076-100	$6.00
101-125	$6.50
126-150	$7.25
151-175	$8.00
176-200	$9.00
201-225	$9.25
226-250	$9.50
251-275	$10.75
276-300	$11.00

PNL-2944
UC-35

CHARACTERIZATION OF AIRBORNE URANIUM FROM TEST FIRINGS OF XM774 AMMUNITION

J. A. Glissmeyer
J. Mishima

R. L. Gilchrist, Project Manager

November 1979

Prepared for the U.S. Army
under U.S. Department of Energy
Contract EY-76-C-06-1830

Pacific Northwest Laboratory
Richland, Washington 99352

NOTICE

The views, opinions, and/or findings contained in this report are those of the author(s) and should not be construed as an official Department of Army position, policy, or decision, unless so designated by other documentation.

PROLOGUE

As stated in the foreward, this study was conducted at the recommendation of the Joint Technical Coordinating Group for Munitions Effectiveness (JTCG/ME) Working Group on Depleted Uranium Munitions. This was the first time that an attempt was made to sample the particulate generated during the impact of a 105-mm depleted uranium kinetic energy penetrator into a NATO heavy triple target.

Much useful data were gathered but unexpected conditions have led to some questionable results beyond the control of the experimenters. These conditions included: (1) particulate samplers became clogged and flow rates went to zero necessitating an estimate of when the filters clogged. The time used influenced the concentrations in Table 6 and the mass of penetrators airborne; (2) cloud films were of poor quality and also were not taken 90 degrees apart which made it difficult to evaluate the cloud volumes, and (3) fallout sampling, Figure 25, was much too sparse close to the target to adequately determine the amount of depleted uranium deposited on the ground.

The mass of penetrator airborne varied from 36 to 104% of the original mass attesting to the problems in 1 and 2 above. Some of the problems were alleviated during the subsequent experiments on the XM735A1. However, it is believed that obtaining a better mass balance during an impact would aid significantly in understanding the hazards of firing DU during testing and wartime. Therefore, it is proposed that additional tests be conducted using an improved experimental design to overcome the problems listed above.

ERNEST W. BLOORE
Chairman
JTCG/ME Working Group on Du Munitions

FOREWORD

This study was conducted at the recommendation of the Joint Technical Coordinating Group for Munitions Effectiveness (JTCG/ME) Working Group on Depleted Uranium Munitions and was supported by the Office of Assistant Project Manager for Tank Main Armament Development, XM1 Tank System, under Army Project Number IL663608D060. The technical monitors were the Working Group Chairman, Ernest W. Bloore, and Edward F. Wilsey, both of the U.S. Army Armament Research and Development Command, Dover, New Jersey.

This study is one of three studies recommended by the JTCG/ME Working Group. The first two studies, Radiological and Toxicological Assessment of an External Heat (Burn) Test of the 105 mm Cartridge, APFSDS-T, XM774,[1] and Radiation Dose Rate Measurements Associated with the Use and Storage of XM774 Ammunition,[2] have been distributed. R. L. Gilchrist served as overall Project Manager for Pacific Northwest Laboratory.

The authors wish to acknowledge the Army Environmental Hygiene Agency for providing meteorological support and the Material Testing Directorate of the Testing and Evaluation Command, especially Mr. K. Ruff for support in conducting the part of the study at Aberdeen Proving Grounds, Maryland.

SUMMARY

Pacific Northwest Laboratory (PNL)[a] conducted experiments at Aberdeen Proving Grounds, Maryland, to characterize the airborne depleted uranium (DU) resulting from the test firings of 105-mm, APFSDS-T XM774 ammunition. The study was conducted at the recommendation of the ad hoc Working Group on Depleted Uranium Munitions of the Joint Technical Coordinating Group for Munitions Effectiveness (JTCG/ME). The goal was to obtain data pertinent to evaluations of human inhalation exposure to the airborne DU. Data was desired concerning the following:

1. Size distribution of airborne DU
2. Quantity of airborne DU
3. Dispersion of airborne DU from the target vicinity
4. Amount of DU deposited on the ground
5. Solubility of airborne DU compounds in lung fluid
6. Oxide forms of airborne and fallout DU.

The experiments involved extensive air sampling for total airborne DU particulates and respirable DU particles both above the targets and at distances downwind. Fallout and fragments were collected around the target area. High-speed movies of the smoke generated from the impact of the penetrators were taken to estimate the cloud volumes.

From the results, it is estimated that roughly 2.4 kg of airborne DU is generated by each test firing. About 75% of the airborne DU was U_3O_8 and 25% was UO_2. Immediately above the targets about half of the airborne DU was respirable, and of that amount 43% was soluble in simulated lung fluid within 7 days. After 7 days the remaining material was essentially insoluble. The particles in the respirable range were predominantly U_3O_8. Iron and traces of tungsten, aluminum and silicon compounds were found in the airborne particles.

(a) PNL is operated for the Department of Energy (DOE) by Battelle Memorial Institute.

Measurements of airborne DU in the target vicinity (within 20 ft) after a test firing showed that personnel involved in routinely changing targets can be exposed to concentrations exceeding recommended maximums. This may have resulted in part from mechanical resuspension of DU from the soil or other surfaces. A study was recommended that includes further air sampling related to occupational exposure, soil sampling and solubility measurements.

CONTENTS

FIGURES

TABLES

1.0 INTRODUCTION

Knowing the characteristics of an airborne material is essential to understand its environmental impact on humans. The objective of this study was to provide data pertinent to the evaluation of human exposures to airborne depleted uranium (DU) generated during the test firings of the XM774 ammunition. The data sought included:

- Size distribution of airborne (DU) particulates
- Quantity of airborne DU
- Dispersion of airborne DU from the target vicinity
- Amount of DU deposited on the ground
- Solubility of airborne DU compounds in lung fluid
- Oxide forms of airborne and fallout DU.

The program of field experiments included the collection of fallout, fragments and total-particulate and particle size-fractionated air samples. This report presents the findings of those experiments relative to the areas listed above.

This study was performed at the Ford's Farm Range at Aberdeen Proving Ground. A diagram of the firing range is shown in Figure 1. The XM774 ammunition was fired from a 105-mm gun at a NATO Heavy Triple Target, a series of three plates, from a distance of 200 m. The plates were inclined at an angle towards the gun so that fragments were deflected towards the ground as the penetrator impacted the plates in sequence. Structures adjacent to the targets housed flash X-ray equipment for recording the penetration through the targets.

The XM774 ammunition consists of a 3.4 kg penetrator body of depleted uranium alloyed with 0.75 percent titanium by weight. A steel-tipped, aluminum windshield, an aluminum tail fin and an aluminum sabot are attached to the body.

A study by Hanson et al.[3] obtained particle size data for the test firings of a smaller caliber DU ammunition. The study also estimated the amount and respirable fraction of airborne DU. Because air sampling in

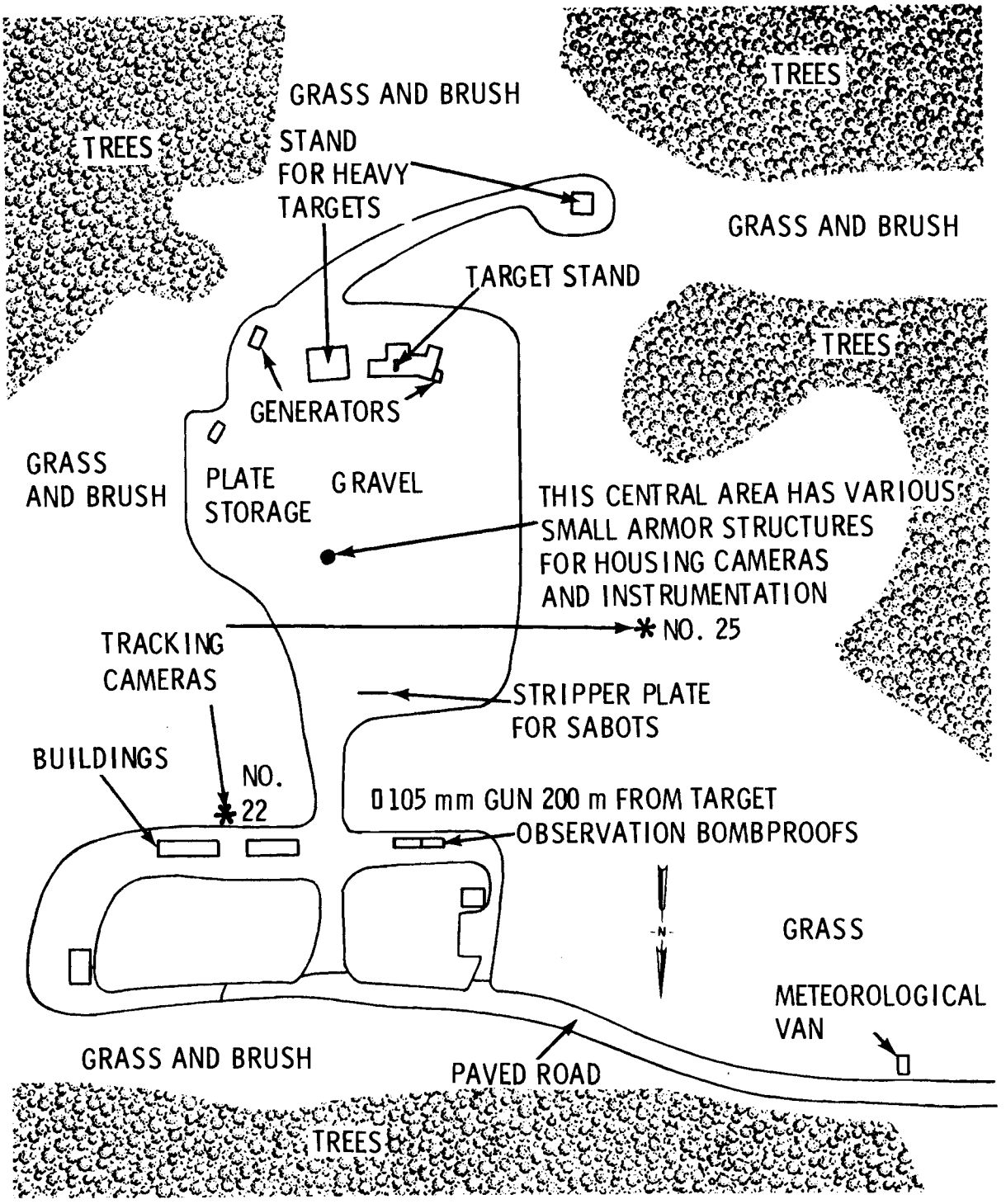

FIGURE 1. Diagram of Ford's Farm Range

Hanson's study was performed using a chamber to enclose the target and the target was different, the results could not be scaled-up to the larger ammunition examined in this study.

2.0 CONCLUSIONS AND RECOMMENDATIONS

From the experiments the following conclusions can be drawn:

1) On the average, approximately 2.4 kg of airborne uranium was generated per test firing of the XM774 ammunition, an estimate that suffers from several uncertainties as discussed in the report. It cannot be concluded how much of the airborne material actually came from the fired penetrator or from resuspended contaminated soil.

2) Roughly one-half of the airborne uranium can be considered respirable.

3) The geometric mean size of the airborne uranium was about 2.5 to 3 μm aerodynamic equivalent diameter.

4) About three-fourths of the airborne uranium was U_3O_8, the other fourth was UO_2.

5) Nearly 43% of the respirable airborne uranium was soluble in 7 days in simulated lung fluid. This result indicates a possible chemical toxicity hazard apart from a radiation hazard.

6) In the personnel accessway adjacent to the target mounts, the concentration of airborne uranium was near or above the occupational Maximum Permissible Concentration (MPC_a) during routine target changing after a test firing. Resuspension of contaminated soil may be a contributor to this concentration.

7) In the same personnel accessway, the airborne concentration was about a factor of two below MPC_a when routine target changing was suspended after one of the test firings.

8) Behind the X-ray film frame adjacent to the target, the measured concentration of airborne uranium was near, or below, that of the accessway and the MPC_a during normal target-changing activity. The concentration in the same location was an order of magnitude lower when target changing was not conducted after one of the test firings.

9) During several test firings the quantity of uranium fallout deposited per firing was about 360 g within 50 ft of the targets. This estimate was

based on the assumption of uniform deposition around each sample; however, there were indications that this assumption may not be true in the area within 10 ft of the target. Additionally, large fragments also contributed to the uranium deposited on the ground, the largest of which weighed about 150 g; however, the large fragments were often scavenged and set aside.

The following are recommended as a result of this study:

1) Investigate the magnitude of the chemical toxicity hazard of the airborne compounds associated with the test firings.

2) More accurately assess the occupational hazard from the test firings. The contribution of resuspended material from contaminated soil to the respirable concentration of uranium should be determined.

3) Consider ways to control the resuspension of deposited airborne material in the target area to minimize personnel hazards.

3.0 DESCRIPTION OF EXPERIMENTS

The experiments conducted to characterize the airborne depleted uranium generated by the five XM774 test firings are described. The experimental methods are described first, then the deployment of sampling equipment during the tests and finally, the analytical methods are outlined.

3.1 SOURCE TERM CHARACTERIZATION EXPERIMENTS

Experiments to characterize the airborne depleted uranium resulting from the test firings were divided into the following tasks:

1. Target-area air sampling
2. Upwind/downwind air sampling
3. Cloud dimensioning
4. Meteorological data collection
5. Target-area airborne-uranium dispersion rate
6. Fallout collection

Time and funds did not permit a detailed dispersion study employing tower-mounted, multilevel air samplers arranged in arcs embracing the cloud. Instead, air samples were obtained from just above the target plates and from a limited number of locations near ground level. Fallout collection was limited to an area within a 50-ft radius of the mounted targets and was collected to allow identification of uranium oxides. The dispersion rate of airborne uranium was to be measured in the immediate target area in order to estimate when personnel could re-enter the area. Methods used in the six tasks are described in detail in the following subsections.

3.1.1 Target-Area Air Sampling

Total particulate samplers were used to estimate the mass of airborne material, and cascade impactors were used to estimate the size distribution of airborne particulates. Six total-particulate samplers and two high-volume cascade impactors were used to collect airborne particulate material in the target area. Each total- particulate sampler consisted of a 2-in., stainless-steel-pipe probe, an in-line 8- x 10-in. filter holder,[a] an

(a) Model IF-2150, General Metal Works Inc., 8368 Bridgetown Road, Village of Cleves, Ohio 45002.

8- x 10-in. rectangle of Whatman 41 filter paper,[a] and a blower.[b] The samplers were set to operate at 50 cubic feet per minute (cfm). A diagram of the total-particulate sampler is shown in Figure 2; an assembled sampler is shown in Figure 3.

Each cascade impactor sampler consisted of a 2-in. stainless-steel-pipe probe, a conical adapter, a high-volume cascade impactor[c] loaded with Whatman 41 substrates and backup filter, a filter holder, and a blower of the type used on the total-particulate samplers. These impactors were operated at 20 cfm. An assembled impactor sampler is shown in Figure 4.

The cascade impactor fractionates the airborne particulates by using aerodynamic properties. The impactor, shown in an exploded view in Figure 5, fractionates particles in four stages, each using a jet plate and a Whatman 41 collection substrate. The four fractionating stages are followed by a backup Whatman 41 filter. The sampled air passes through a jet plate at a velocity determined by the sampling rate and the jet dimensions. Particles with sufficient inertia are impacted on the substrate and the smaller particles pass on to the next jet plate. The stages are ordered so that progressively smaller particles are impacted in the later stages. The backup filter captures the remaining fine particles not impacted on the stages.

Since size fractionation depends more on the aerodynamic behavior of a particle than on its physical size, each stage has a calibrated aerodynamic equivalent cutoff diameter, and the material collected on the impaction substrate has that same mean aerodynamic equivalent diameter (AED).[d] Analysis of the materials collected on each impactor surface and on the backup filter can help reconstruct the size distribution of the aerosol particles in terms of AED.

(a) Whatman Inc., 9 Bridewell Place, Clifton, New Jersey 07014.
(b) Model GMWL-2000, General Metal Works Inc.
(c) Andersen High-Volume Cascade Impactor Model 65-800, Andersen Samplers Inc., 4215-C Wendell Drive, Atlanta, Georgia 30336.
(d) The aerodynamic equivalent diameter (AED) is the diameter of a hypothetical particle of density 1 g/cm^3 with aerodynamic behavior identical to that of the actual particle. For spherical particles, AED = diameter x $\sqrt{\text{specific gravity}}$.

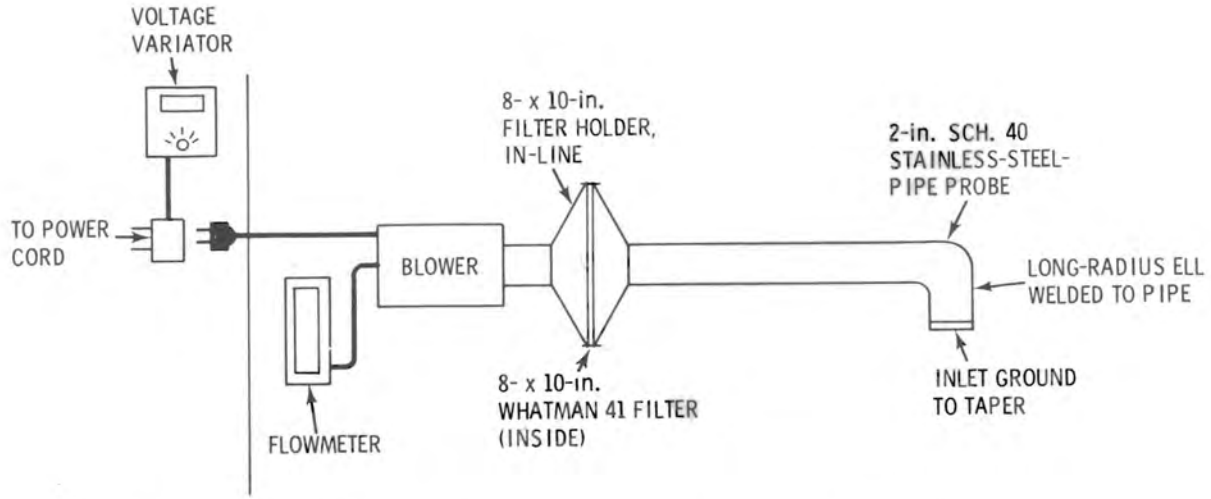

FIGURE 2. Diagram of Total-Particulate Sampler for Target Area

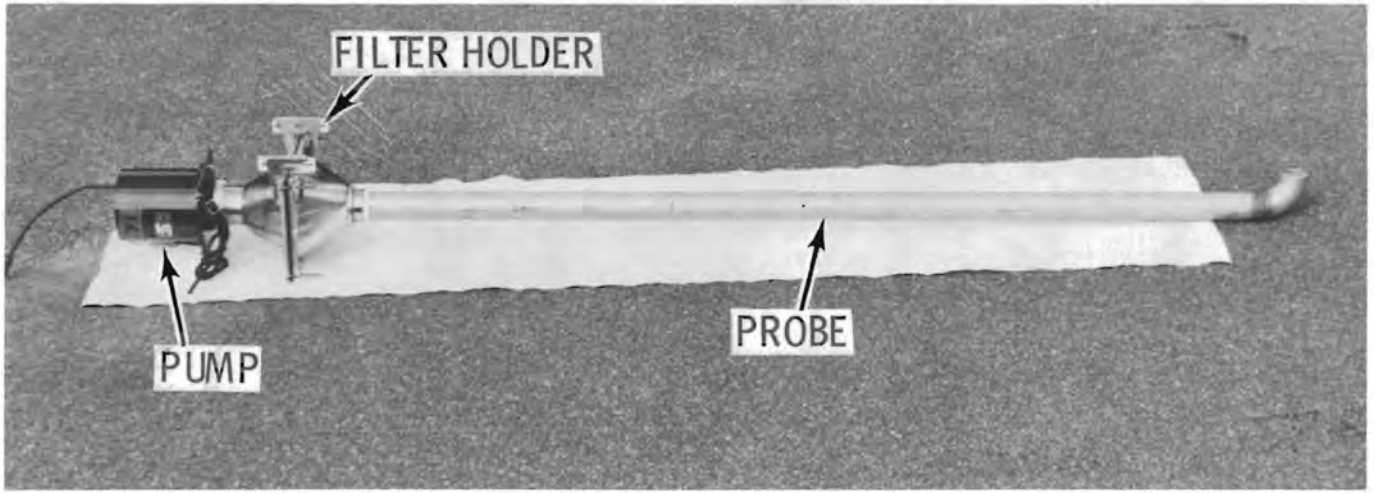

FIGURE 3. Assembled Total-Particulate Sampler for Target Area

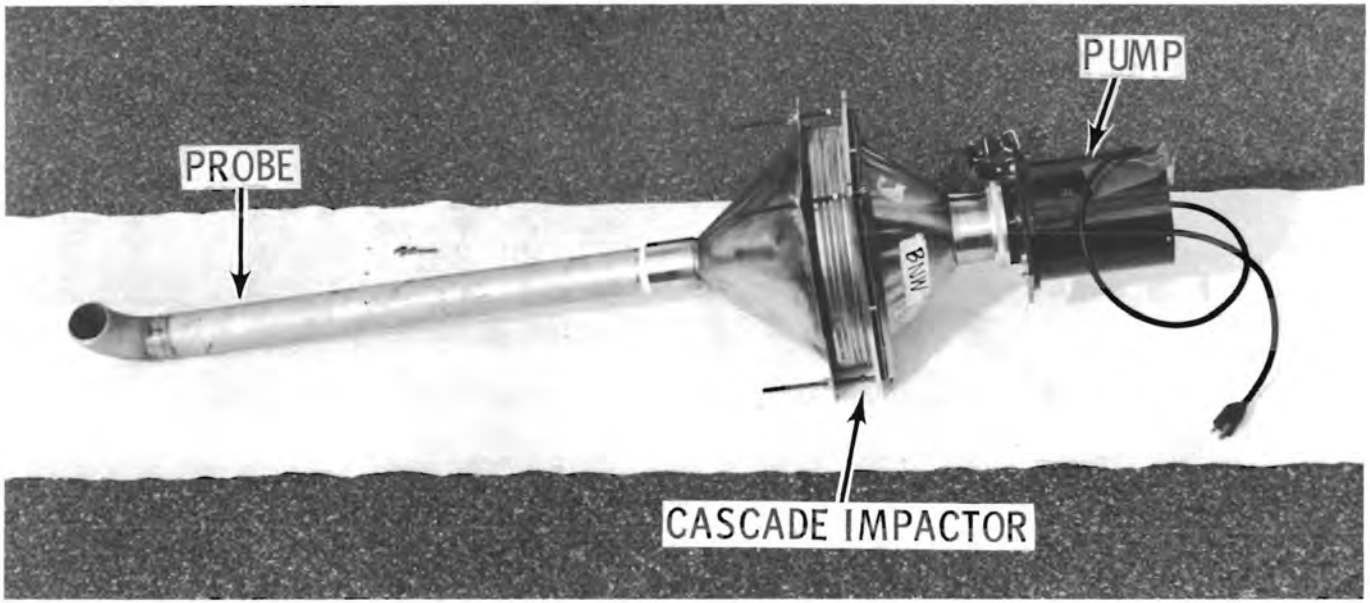

FIGURE 4. Assembled High-Volume Cascade Impactor for Target Area

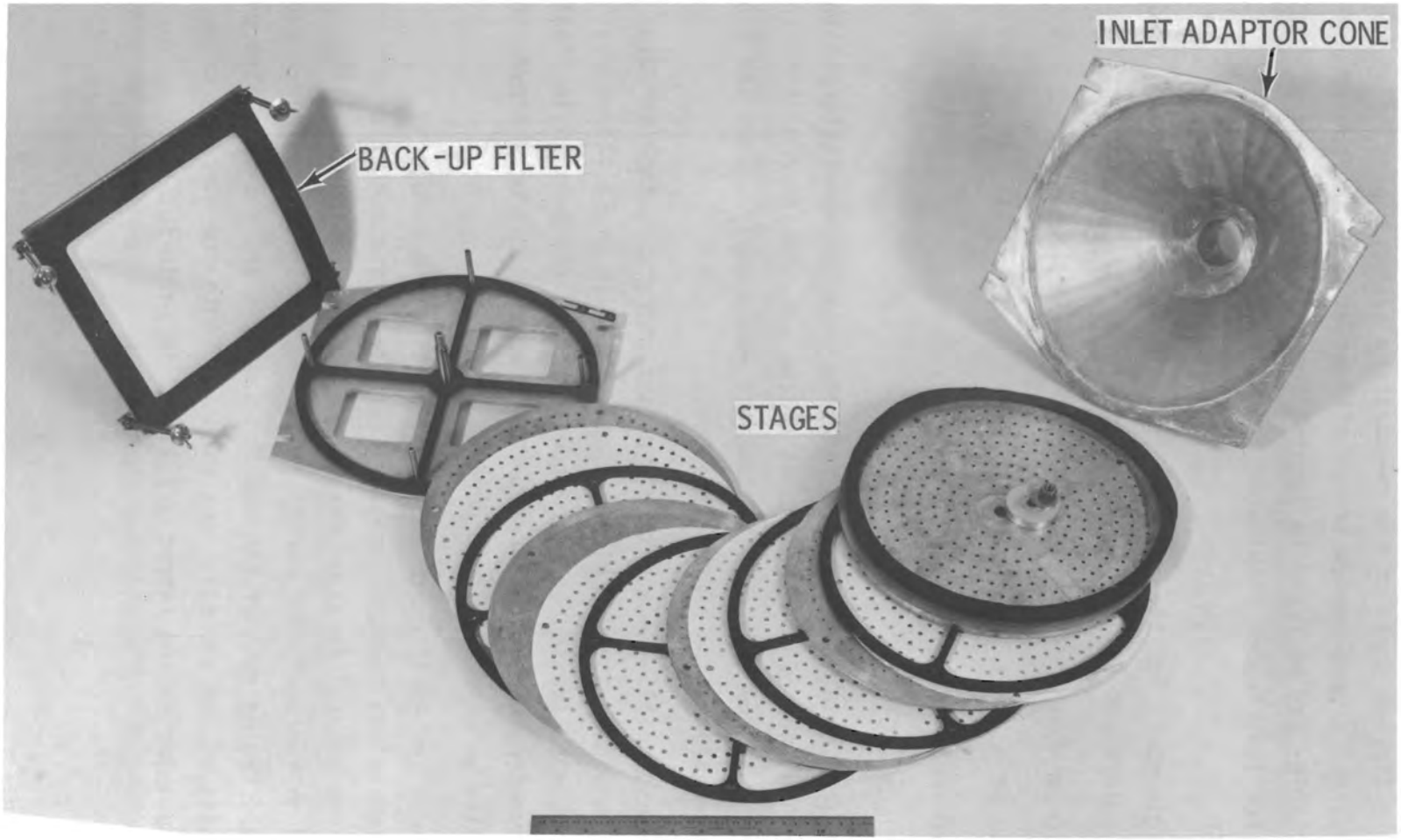

FIGURE 5. Exploded View of Anderson Model 65-800 Four-Stage High-Volume Cascade Impactor

Measuring particle size by its AED is useful becauses inhaled particles are deposited in different parts of the respiratory system depending on their aerodynamic behavior. A good review of definitions of what are considered "respirable" particles can be found in Aerosol Technology in Hazard Evaluation.[4] For this report respirable particles will be defined as those ≤ 3.3 μm AED.

The cutoff diameters for the impactor (four fractionating stages) used in this study were determined using glass-fiber media substrates and are:

- Stage 1--7.0 μm AED
- Stage 2--3.3 μm AED
- Stage 3--2.0 μm AED
- Stage 4--1.1 μm AED

It was felt (following consultation with the impactor manufacturer) that the thickness and texture of the Whatman 41 filter was similar enough to the glass-fiber media that the same cutoff diameters would apply. Time and funds did not permit a recalibration of the impactor.

The flow rates for all the samplers were set using a voltage variator to control the vacuum blower speed. Flow was measured with small flowmeters calibrated against a calibrated orifice made to fit on the 8- x 10-in. filter holder. The flowmeters were recalibrated during spot checks or whenever the adjusting mechanism was knocked loose during a run.

Figure 6 shows the location of the total-particulate samplers (T_1 - T_6) and high-volume cascade impactors (I1-I2) in the target area; the probes were set about 2 ft above the tops of the target plates. The samplers mounted on the bombproof had 61-ft probes; those on the film-frame had 2½-ft probes. Photographs of the mounted samplers are shown in Figures 7, 8, and 9. Examples of the abbreviations used to denote the samplers shown in these figures and later in the report are listed in Table 1.

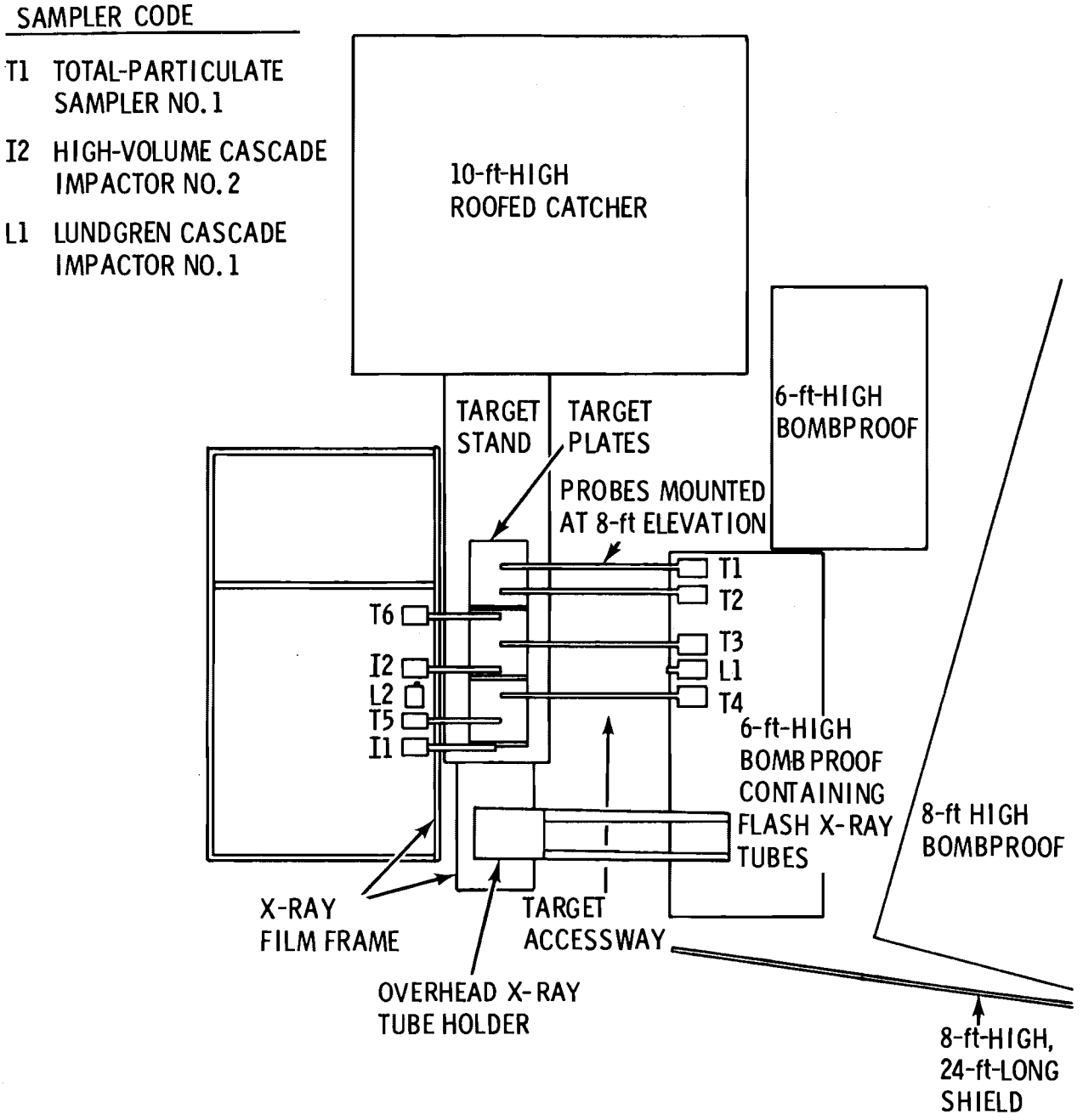

FIGURE 6. Plan of Sampler Array in the Target Area of the Ford's Farm Range

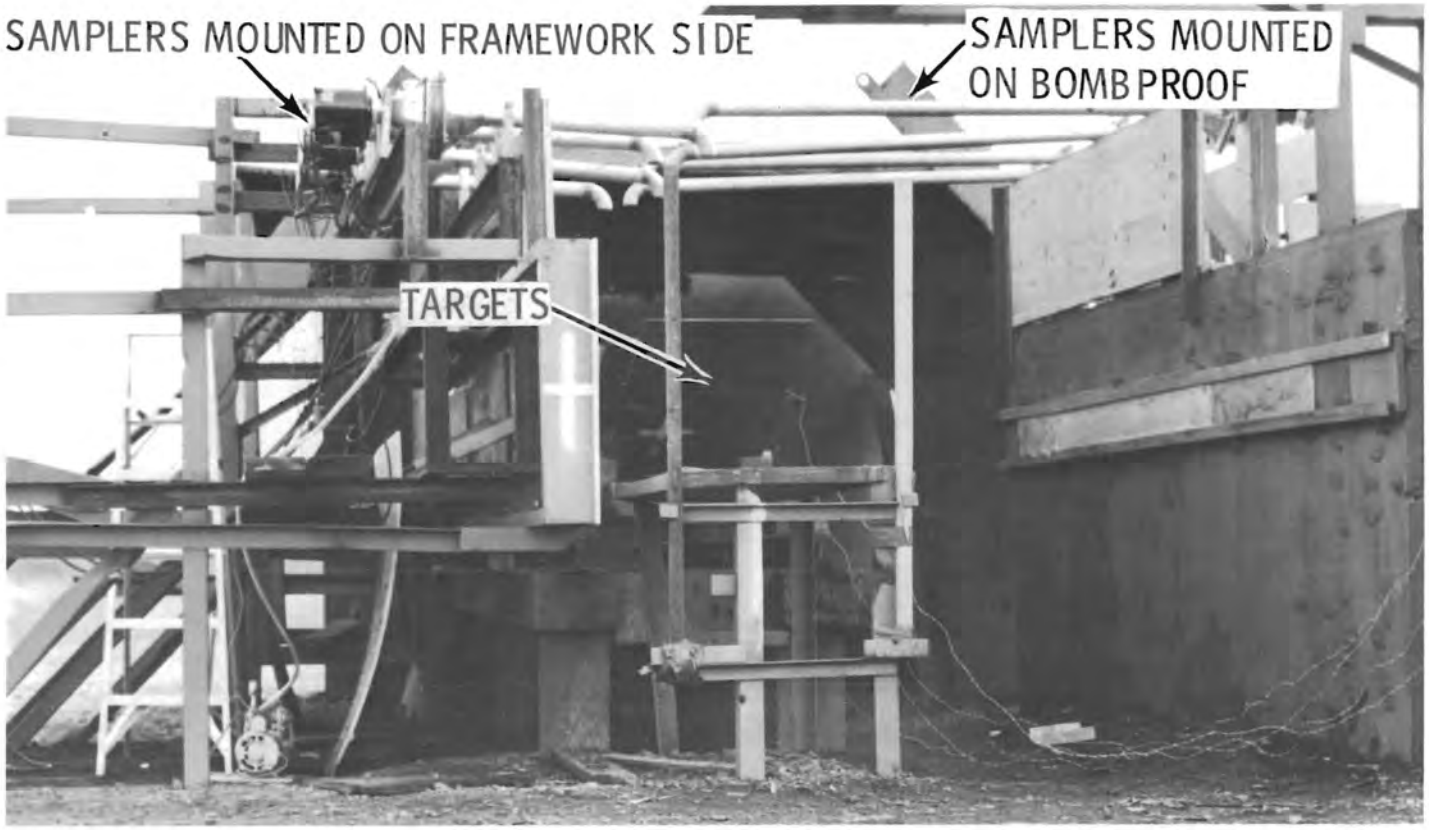

FIGURE 7. Target Showing Probes of Samplers T1-T6 and I1, I2. (Probes are positioned about 8 ft above grade.)

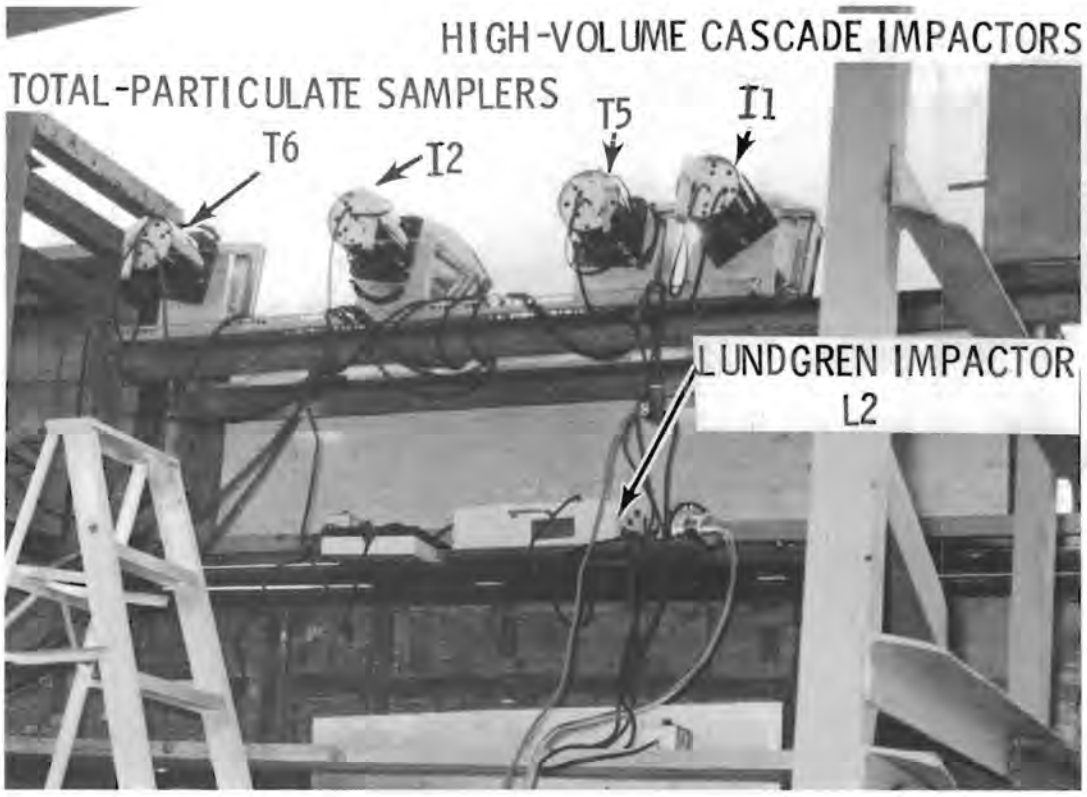

FIGURE 8. Rear of Film Frame Showing Samplers I1, I2, T5, T6, and L2.

TABLE 1. Sampler Abbreviations

T1 - 8- x 10-in. total-particulate sampler No. 1
I2 - High-volume cascade impactor No. 2
L2 - Lundgren impactor No. 2
S3 - Staplex total-particulate sampler No. 3

Isokinetic sampling[(a)] was not attempted in this study The authors expected the velocity and direction of air in the sampling area to vary rapidly, and it was impractical to control the sampling rate as rapidly. Therefore, the size distribution of the collected samples is probably not ideally representative of the airborne particulates.

(a) That is, maintaining an air velocity in the probe nozzle identical to the velocity of the approaching air, one of the measures required to assure that the size distribution of particles in the sample is identical to that in the air being sampled.

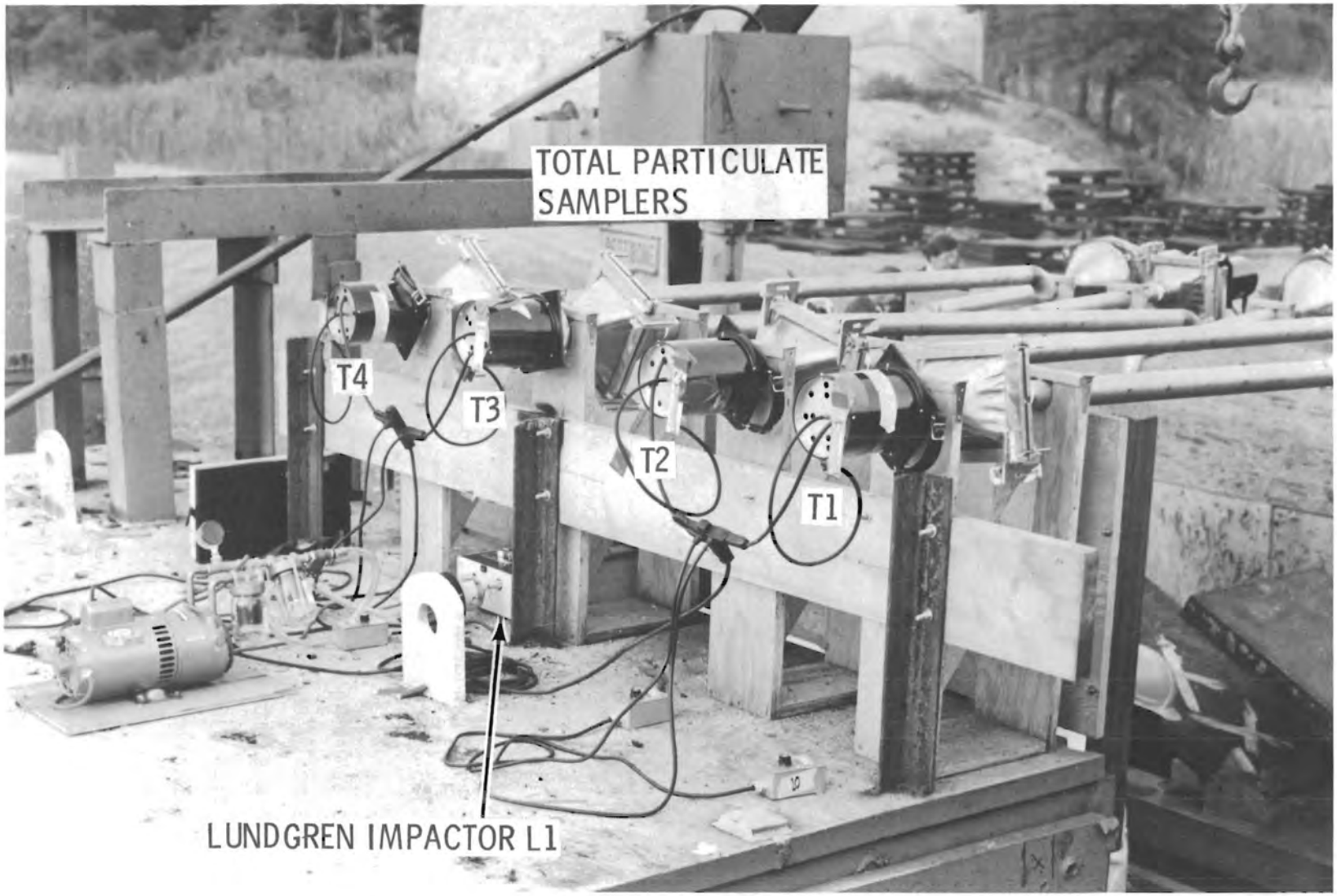

FIGURE 9. Rear View of Samplers Mounted on Bombproof

3.1.2 Upwind/Downwind Air Sampling

Upwind and downwind air sampling was attempted within a 150-ft radius of the targets and at selected locations in the Industrial Area at Aberdeen Proving Grounds. All samplers were located in clearings and placed 4 to 6 ft above grade. The samplers used were high-volume cascade impactors and total-particulate samplers with 4-in. diameter and 8- x 10-in. filters.

Two high-volume cascade impactors were set up for each run, one located upwind and one downwind from the target area. This equipment was identical to that used in the target area, except that 1) there were no inlet probes, and 2) the impactors were mounted with the plane of the jet plates horizontal and the intake side facing up.

Two total-particulate samplers with 8- x 10-in. filters were set up for each run, one upwind and one downwind from the target area. These samplers were identical to the target area's total-particulate samplers except that they were 1) mounted so that the filter was oriented horizontally and 2) had no inlet probe. The samplers were mounted on aluminum shelters, with Whatman 41 filters exposed to the atmosphere. Flow rate was controlled and calibrated as in the other tests.

High-volume total-particulate samplers with 4-in.-diameter filters[(b)] were provided by Army Armament Research and Development Command (ARRADCOM). Three to five of these samplers were deployed for each run: one was located at the Human Engineering Laboratory (HEL) field and one at the Mile Test Loop (MTL) in the Industrial Area as indicated in Figure 10. The others were located in the upwind and downwind sampler groups. During the course of the experiments, some sampling was conducted by the Army at the Building 938 and Michaelsville locations, also shown in Figure 10. The deployment of the Staplex samplers varied from run to run and will be described in Appendix A.1.

Each Staplex unit had a built-in flowmeter, and three of these units had marked flow calibrations for Whatman 41 filters. These units, designated S1, S2, and S3, were marked as follows:

(b) The Staplex Company, 777 Fifth Avenue, Brooklyn, New York 11232.

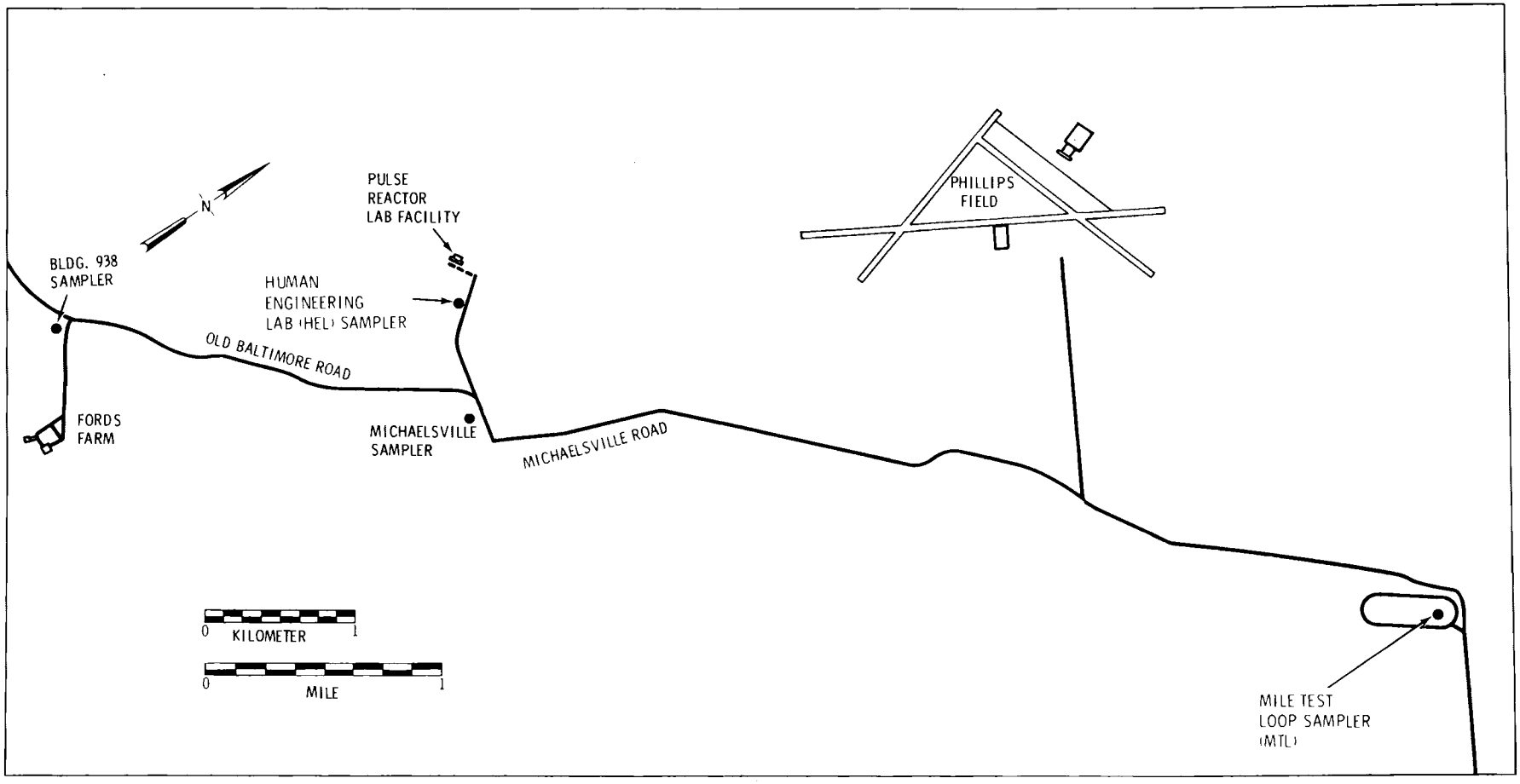

FIGURE 10. Position of Auxiliary Samplers Relative to Ford's Farm Firing Range (to scale)

Unit	Flow Rate, cfm
S1	24.75
S2	26.1
S3	25.88

The flow rates of the other units were read from their flowmeters without a calibration check.

The upwind and downwind sampler groups used for Run 1 are shown in Figures 11 and 12.

3.1.3 Cloud Dimensioning

The measurements of cloud dimensions and rise time were made from high-speed motion pictures provided by the U.S. Army Testing and Evaluation Command (TECOM). Still photography and some color movie footage were also provided.

The high-speed motion pictures were taken in black and white using two tracking cameras separated by an included angle of about 57 degrees and located about 200 m from the target area (see Figure 1). The measurements made from these films aided in determining the source term for airborne uranium. The total airborne uranium was approximated from the concentrations measured in the target area and from the size of the cloud.

3.1.4 Meteorological Data Collection

Meteorological support for this project was provided by the U.S. Army Environmental Hygiene Agency (AEHA). A mobile meteorological system was located approximately 500 m from the target area in an open field (see Figure 1).

The windspeed, wind direction, and standard deviation of the wind direction were measured at 10 m above grade. Solar radiation and ambient temperature were also measured. The stability category was estimated using the Brookhaven Stability Class system.[5] All meteorological data were reported as 5-min averages for the periods from about 30 min before to 60 min after each test firing for which target area and upwind/downwind samplers were operated. Otherwise, the meteorological data were reported as 1-hr averages

FIGURE 11. Upwind Samplers Located about 80 ft from Target (Run 1)

for all time periods between October 4, 1977 (1430 hours) and October 9, 1977 (1000 hours). Appendix A.2 contains meteorological data extracted from the AEHA report.

3.1.5 Target-Area Airborne-Uranium Dispersion Rate

The rate of dispersion of airborne uranium in the target area was determined using Lundgren Cascade Impactors[a]. The principle of aerodynamic fractionation of airborne particles is the same as discussed earlier; however, features of this impactor make it useful for this

(a) Lundgren Impactor Model 4220, Environmental Research Corp. St. Paul, Minnesota; now marketed by Sierra Instruments, Inc.

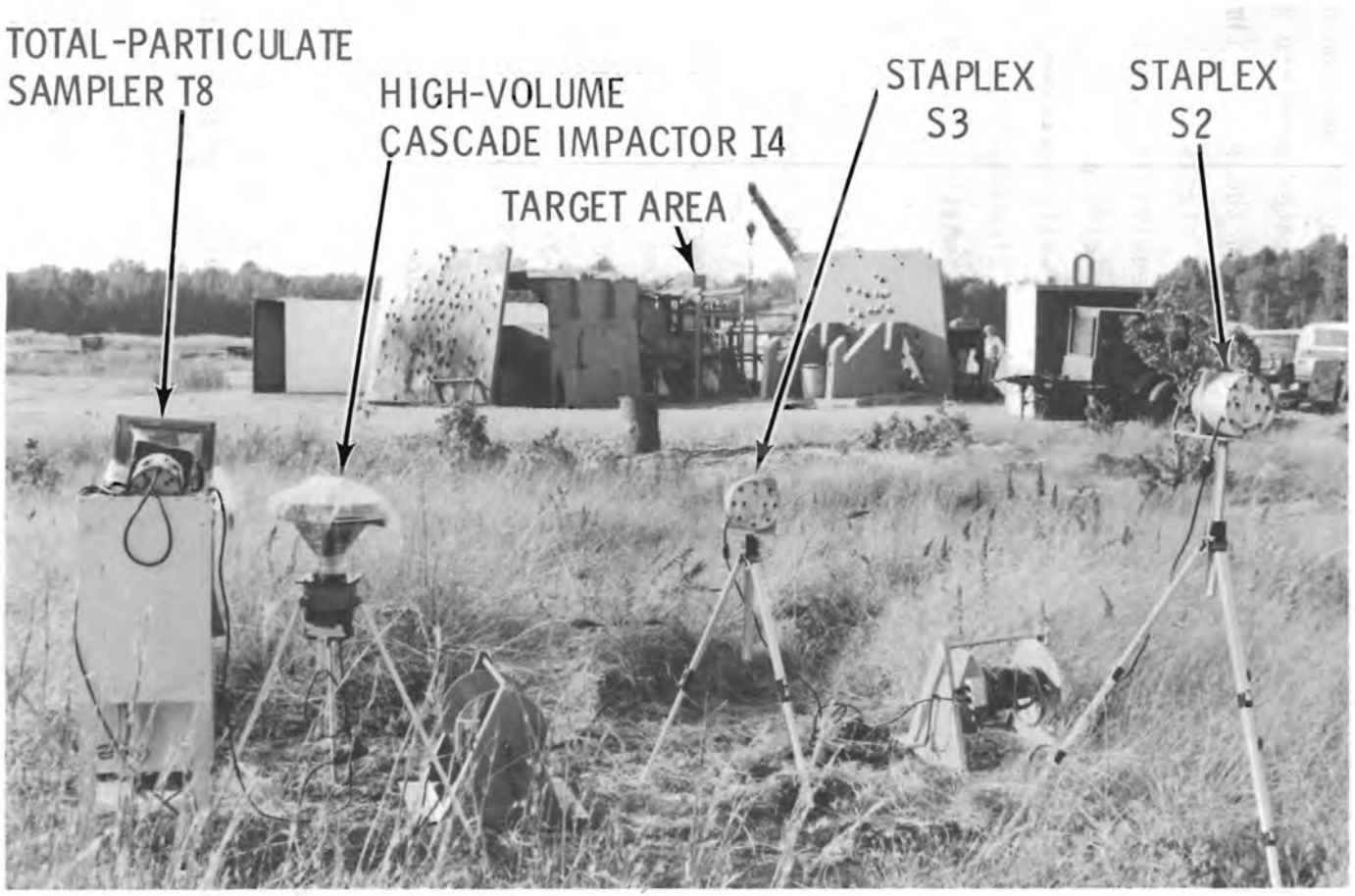

FIGURE 12. Downwind Samplers Located about 145 ft from Target (Run 1)

experiment. Instead of a circular plate with many jets at each stage, the Lundgren impactor employs a single rectangular jet at each stage. The impaction substrate is a thin rectangular film of mylar instead of Whatman 41 filter. The mylar film is wrapped around a cylinder that rotates past the jet at selectable speeds. Thus, the location of the particles on the mylar film can be related to the time of sampling. There are four such stages in the Lundgren impactor, each with a characteristic aerodynamic equivalent cutoff diameter[(a)]. A backup filter follows the four stages and yields a time-integrated rather than a time-dependent sample. An MF-Millipore membrane filter[(b)], with a high collection efficiency for submicron airborne particles, was used as a back-up filter. Figure 13 is a schematic drawing of the Lundgren impactor.

A thin coating of grease was rubbed onto the mylar substrates after they were mounted on the cylinders to increase particle adhesion and decrease large particle bounce. This practice was satisfactory for all but the fourth stage. The clearance between the cylinder and jet of the fourth stage was so small that, in some cases, the coating rubbed and smeared the deposited particles. The stretch of the mylar substrate contributed to the problem because the substrate did not always fit the cylinder tightly.

The vacuum source for the impactor was a sliding vane pump. A photograph of the assembled sampler is shown in Figure 14. The flow rate was set at 3 cfm as indicated on the impactor's built-in calibrated flowmeter.

The impactors were located in areas close to the targets where personnel perform most of their tasks. Lundgren L1 was located on the bombproof and sampled from the target accessway (the walkway between the targets and the bombproof) at a 6-ft elevation above grade. Lundgren, L2, was located on the framework where the X-ray film was mounted (see Figure 6).

(a) Stage 1--9.4 μm AED
Stage 2--2.8 μm AED
Stage 3--0.9 μm AED
Stage 4--0.26 μm AED

(b) MF-Millipore is a filter made of mixed cellulose esters.

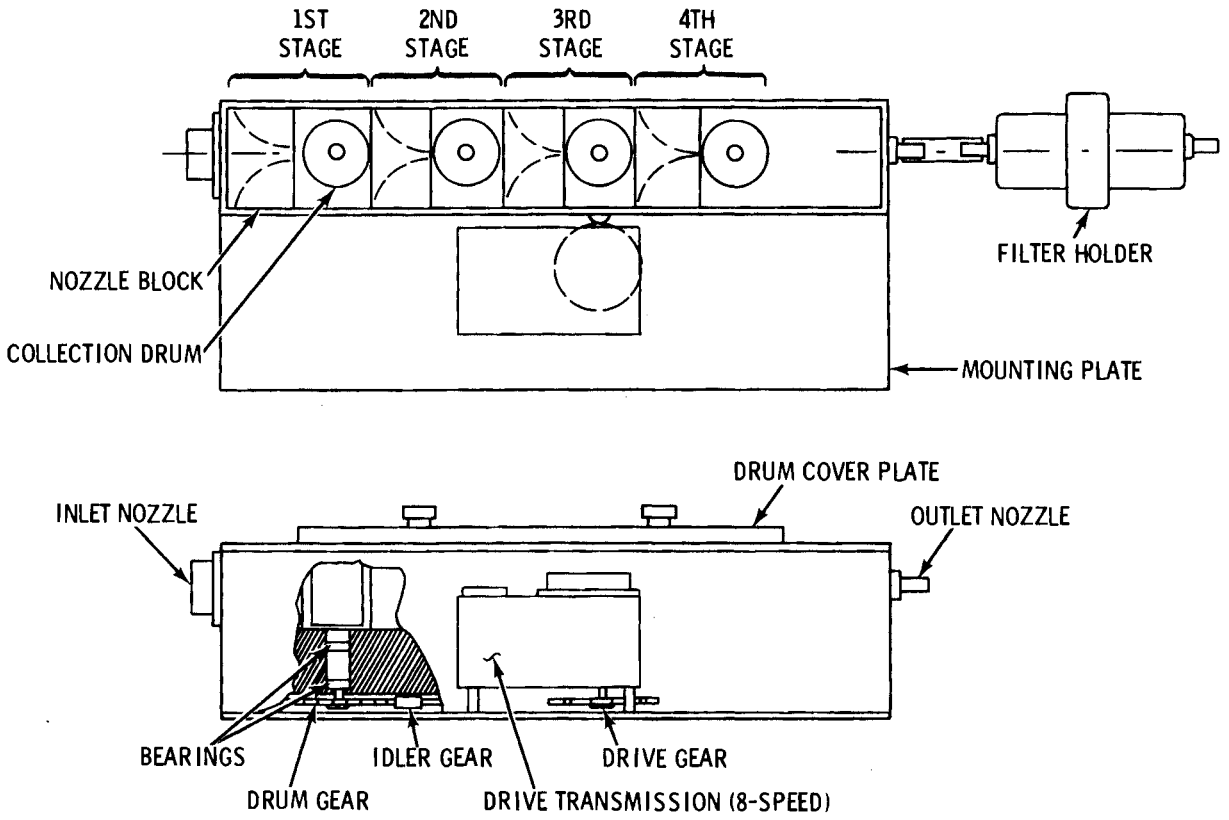

FIGURE 13. Schematic Diagram of Lundgren Impactor

3.1.6 Fallout Collection

Two plans were used to collect fallout. One was to collect sufficient fallout for the identification of uranium oxides. For this purpose, stainless-steel trays, 8 x 11 in., were set out for a test firing, then covered and moved during the changing of targets. These trays were located where small fragments of depleted uranium had been found. The layout of the trays is shown in Figure 15. The samples from this experiment will be referred to as the "dry fallout" samples.

The second plan was designed to estimate the amount of uranium fallout within a 50-ft radius of the targets. Three-quart Pyrex trays containing water were used to collect the fallout. (The water made it easier to transfer the collected particles to sample jars.) The tray layout is shown in Figure 16. The area included in a 50-ft radius from the center of the middle target was divided into three annular and one circular region, all of equal area. The two inner regions were divided radially into sixths. A tray was

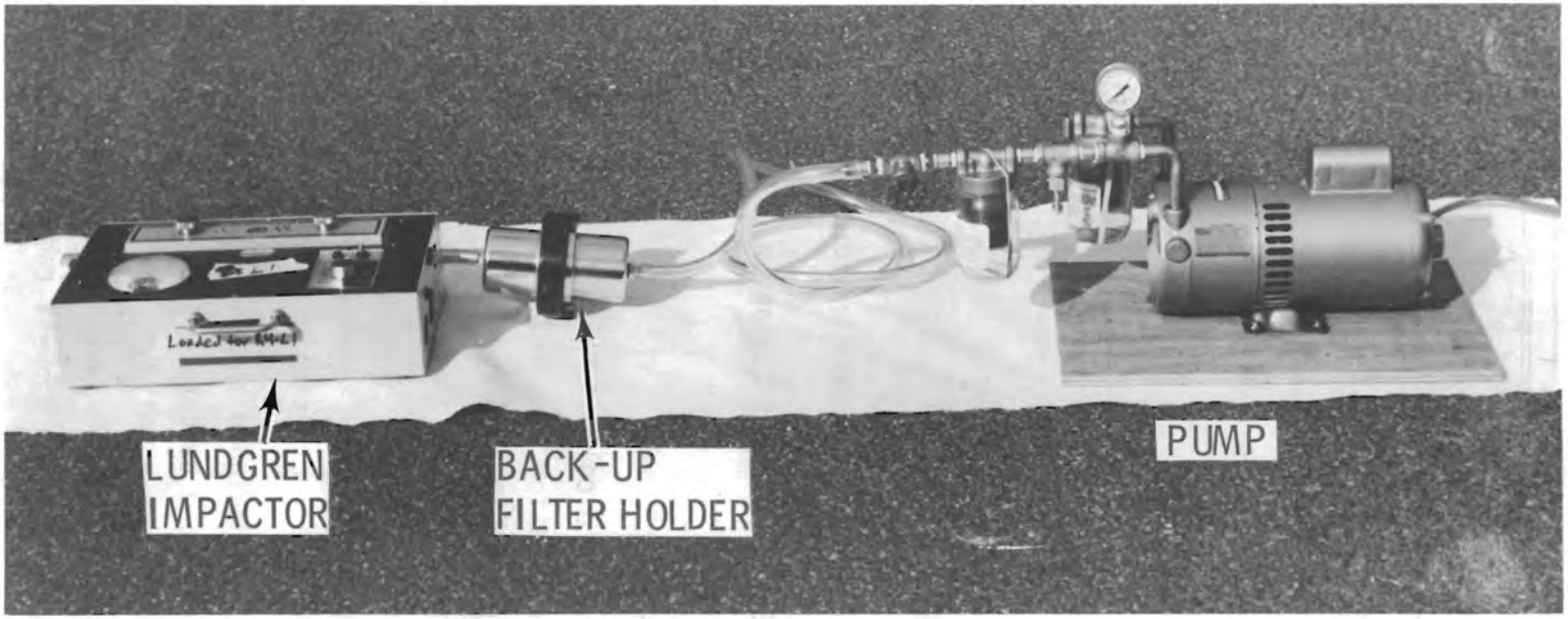

FIGURE 14. Assembled Lundgren Impactor Sampler

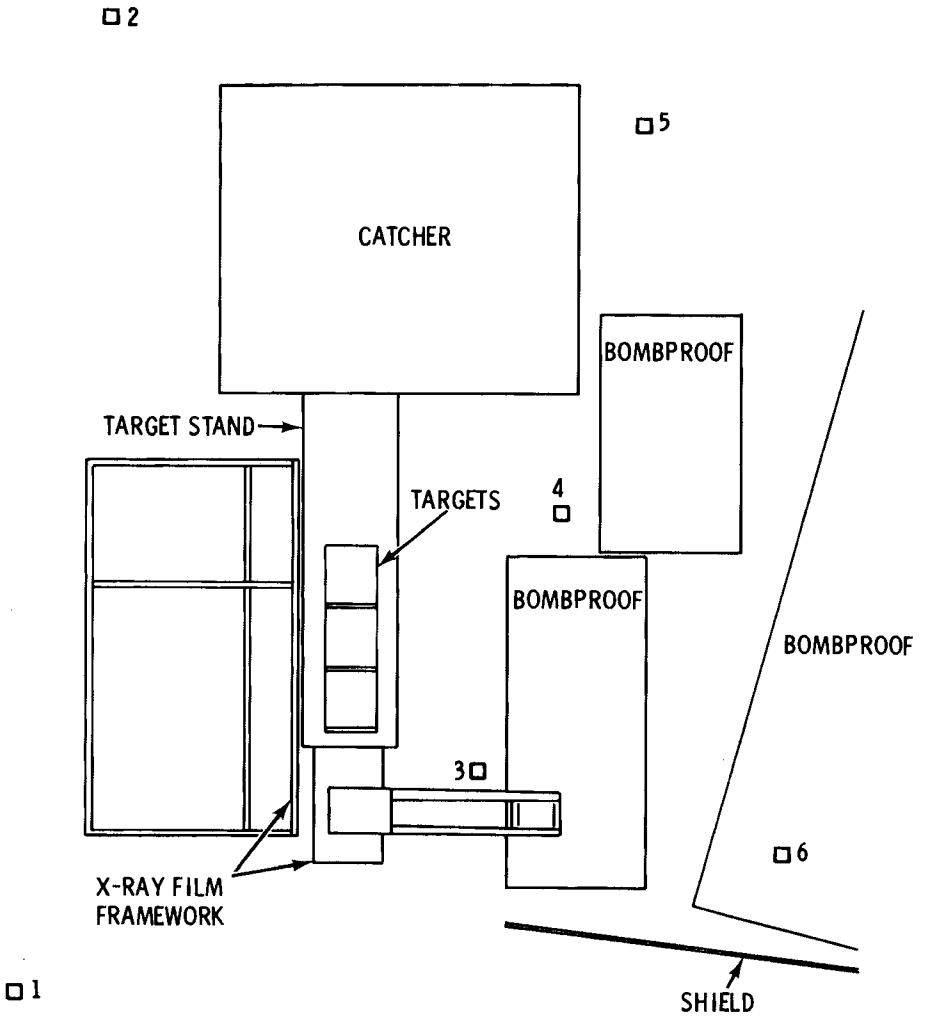

FIGURE 15. Approximate Locations of Dry Fallout Trays

located in each of the 12 areas, and the amount of fallout collected in each tray was considered representative of the 327-ft^2 area. The two outer regions were divided radially into quarters. A tray was located in each of the eight equal areas to represent the 490-ft^2 area. Each tray was located in the centroid of its region. The equation for the region radial boundaries is included in Figure 16. The samples from this experiment will be referred to as the "wet fallout" samples.

3.2 EXPERIMENTS

The experiments performed during the test firings will be outlined in this section. Details concerning the operation of air samplers are discussed in Appendix A.1.

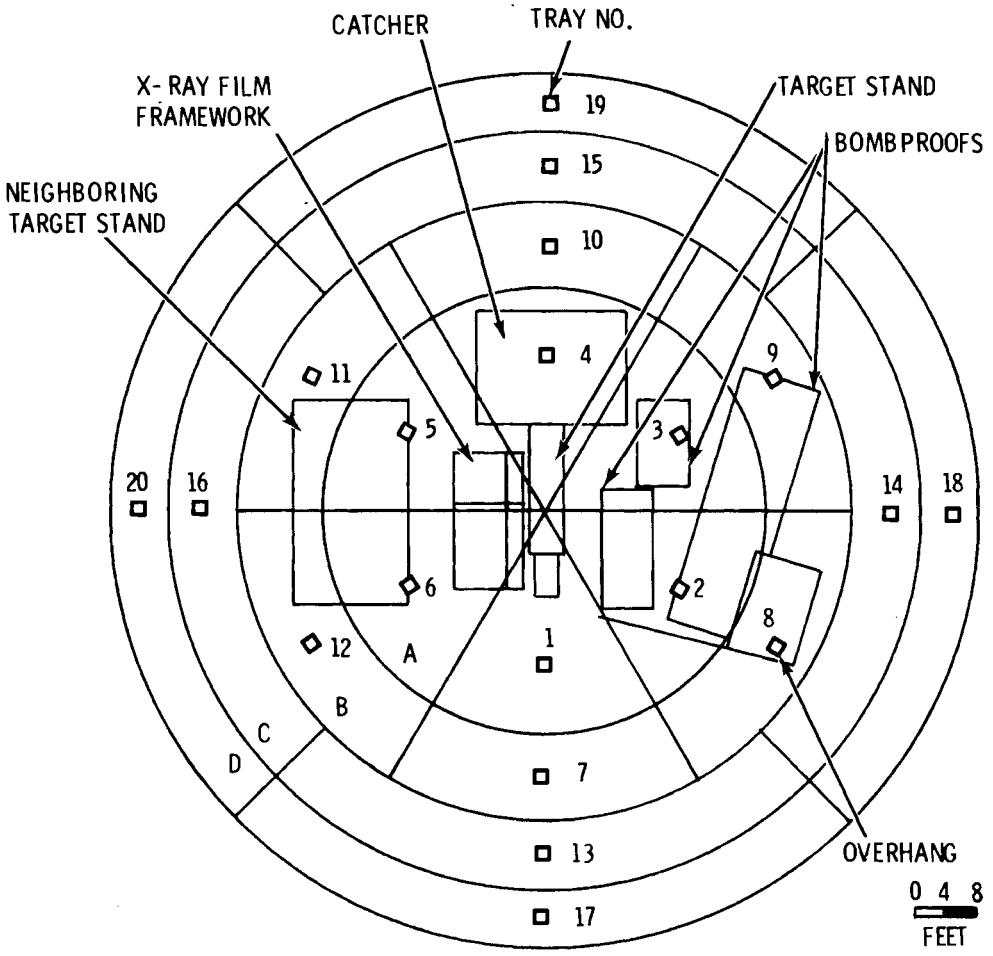

TRAYS 2, 3, 4, 8 AND 9 ON STRUCTURES

AREA BOUNDARY RADII $R_N\sqrt{\frac{na}{\pi}}$

R_A = 25 ft
R_B = 35.4 ft
R_C = 43.3 ft
R_D = 50 ft

□ 21 BY STORAGE BUILDINGS UPRANGE
□ 22 IN LAB, CONTROL

FIGURE 16. Layout of Water-Filled Fallout Trays

3.2.1 Air Sampling

The air sampling experiments were repeated five times. The equipment was set up at the firing range while the range crew prepared the targets for the test firing. After the samplers were in place, the X-ray crew mounted the X-ray films. The samplers were started and set to their required flow rates, and all personnel took cover in the bombproofs near the gun (see Figure 1). After the firing, personnel were required to wait 15 min before entering the target area. After the waiting period, the air sampler flow rates were checked before being shut off at the desired times.

Generally, after the shot the upwind/downwind and Lundgren impactor samplers were operating at their set flow rates. If they were to be left on for an extended time, they required only minor adjustment. However, the target-area total-particulate and high-volume impactor samplers were all found operating at drastically reduced flow rates after the shot. The flowmeters could not be read in most cases because the flow was below scale (below 5 cfm). Therefore, the airflow and sampling duration of these air samplers can only be estimated.

The upwind and downwind sampler groups were located 90 to 150 ft from the target stand. It was difficult to judge wind direction because it changed frequently and the wind speed was low (<5 mph). In some cases, the wind shifted 180^{o} between the time the equipment was set up and the time the round was fired. The samplers at HEL and MTL were set up and operated for most runs. They were operated unattended for up to 12 hr.

The operation of the air samplers during each test firing is detailed in Appendix A.1. Figures showing the arrangement of upwind/downwind samplers with respect to the targets and the observed meteorological conditions for each test firing are also found in Appendix A.1.

3.2.2 Fallout Sampling

"Dry fallout" was collected in stainless-steel trays (see Figure 14) on October 6 and 7, 1977, during the nine test firings listed in Table 2. On

TABLE 2. Firing Times During Which Fallout Was Collected

Dry Fallout			Wet Fallout	
October 6		October 7	October 8	
0951	1421	1401	0850	1451
1056	1505	1508	1048	1339
1143	1722		1203	1603
1330				

October 6, the trays were out for seven test firings in rainy conditions. The wet material collected was scraped off the trays and combined into one sample; paper towels used to wipe the trays were added to the sample. The trays were then cleaned for the next day.

On October 7, the trays were set out in the same pattern as before but for only two test firings. This time the material collected was dry and was brushed off the trays and again combined into one sample. The samples collected on both days contained wood chips and soil.

The water-filled fallout trays were set out on October 8 according to the pattern shown in Figure 15 and during the firings listed in Table 2. The contents of each tray were washed into labeled plastic jars.

3.3 SAMPLE ANALYSIS

Four types of sample analyses were completed for this study: 1) total uranium content by gamma spectroscopy, alpha counting or fluorometry; 2) total uranium by X-ray fluorescence; 3) uranium solubility in simulated lung fluid; and 4) uranium oxide analysis by X-ray diffraction and scanning electron microscope. The disposition of the various sample types into these analytical categories is summarized in Table 3. The procedures employed for handling air samples in the field are outlined in the following subsection. Then, further sample preparations and analytical methods are briefly described. Details for each procedure are found in the appendices.

TABLE 3. Summary of Disposition of Samples

	Oxide Analysis & Morphology Electron Microscope[a]	Total Uranium Analysis[b]	Total Uranium X-ray Fluorescence[c]	Solubility[d]
Target-Area Total Particulate	1/16th Fraction of 6 Filters	1/4 Fraction Plus Probes	---	Fraction of 5 Samples
Other Total Particulate	---	1/4 or 1/2 Fractions	---	
Target-Area High-Volume Impactor	Fraction of 2 Impactors	1/4 Fractions Plus Swabs	---	Fractions of Same Impactors Used for Oxide Analysis, Stages 3,4 and Filter
Other High-Volume Impactor	---	1/4 Fractions Plus Swabs	---	Fraction of One Impactor Stages 3,4 and Filter
Lundgren Backup Filter	---	All	---	---
Lundgren Substrates	---	---	All	---
Dry Fallout	---	Fractions	---	---
Wet Fallout	---	All	---	---

(a) Metallurgy Research and Analytical & Nuclear Research Sections, PNL.
(b) U.S. Testing, Richland Division.
(c) Chemical Methods and Kinetics Section, PNL.
(d) Inhalation Technology & Toxicology Section, PNL.

3.3.1 Field Handling of Air Samples

The filters from the total-particulate samplers were removed, folded, bagged and labeled. The probes were removed, washed repeatedly with distilled water, and swabbed with moistened cellulose tissue. The washings and swabs were combined as one sample.

For the target-area high-volume cascade impactors, the probe, inlet adaptor, and face of the first jet plate were washed and swabbed. This was termed the "probe" sample. For the other high-volume impactors, the face of the first jet plate was swabbed and the swabs were saved as a sample. From then on, the cascade impactors were all treated identically. The first jet plate was removed, and the perforated substrate beneath it was folded and bagged. The bottom of the first jet plate and the top of the second plate were swabbed, and swabs were added to the perforated substrate. This procedure was repeated for each successive stage and for the back-up filter.

The mylar substrates of the Lundgren impactors were removed from each drum, taped to cards and placed in containers so that the deposited materials would not contact other surfaces. The backup filter was folded and bagged. The holder for the backup filter was swabbed and the swabs were placed with the filter.

3.3.2 Uranium Analysis Procedures

Analyses for uranium in most samples were performed by United States Testing Company (UST) in Richland, Washington. The total-particulate, high-volume cascade impactor, Lundgren impactor backup filter, and fallout samples were analyzed for total uranium. The preparation of the samples for analysis is detailed in Appendix B.1.

Because of a lack of funds, not all of the upwind impactor samples were analyzed. However, it was felt that they would not add significantly to our findings because they were probably not located far enough upwind of the targets to give a true background uranium size distribution. Because of the diffusion from the rapidly expanding cloud following the impact of the ammunition, the upwind samplers were possibly contaminated (see pp. 44-46).

UST used three methods to determine the uranium content of the samples: gamma spectroscopy, alpha counting and fluorometry. A simplified flow chart of the methods is shown in Figure 17.

Gamma counting was used only for samples that gave hand-held geiger counter readings distinguishable from background. The analysis for uranium was based on the assumption of equilibrium between thorium-234 and its parent uranium-238 and on the isotopic content of the ingot from which the penetrator was made.

Most of the filter, substrate and liquid suspension (probe wash and some "wet fallout") samples were processed through pyrosulfate fusion to ensure dissolution of all particulates. The uranium was then extracted from the solution with hexone. A portion of the extractant solution was plated on a planchet and subjected to an alpha-counting technique. Those samples for which the counting statistics were unacceptable were subjected to analysis by fluorometry. A portion of the hexone extractant was fused into a pellet of NaF-LiF for the fluorometric analysis.

3.3.3 Lundgren Impactor Substrates

The four Lundgren cascade impactor substrates from one impactor are shown in Figure 18. The dark bands are deposits of particles collected when the concentration of airborne particles was particularly high. Substrate 4 shows how the deposits on this stage were frequently smeared in the impactor.

Each substrate was cut vertically into segments (see Figure 18) representing intervals of sampling time. Each segment was then analyzed for uranium using an X-ray fluorescence technique. The uranium content of the four segments (for example, the four labelled "A") corresponding to the same time interval were summed, and a weighted amount of the uranium on the backup filter was then added to the sum to estimate the total uranium collected during the time interval. The details of sample preparation and some sample calculations are included in Appendices B.2 and B.3.

3.3.4 Oxides

The relative abundance of uranium oxides made airborne during the test firings was determined semi-quantitatively by X-ray diffraction analysis of portions of target-area total-particulate sample filters (one from each test

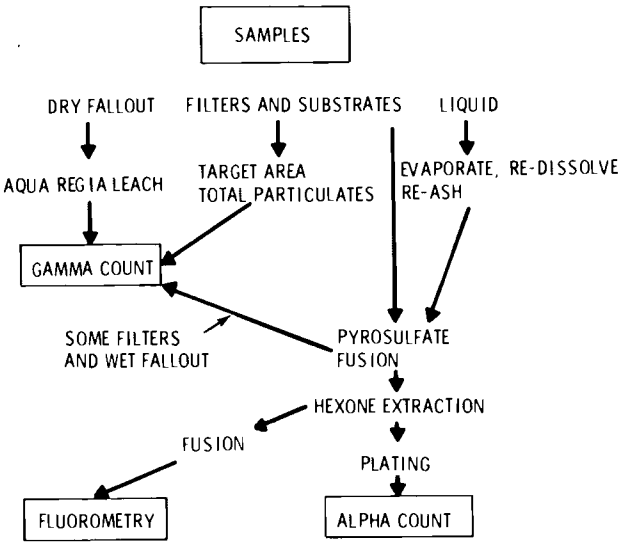

FIGURE 17. Simplified Flow Chart for Uranium Analysis

firing). The same analysis was made for fractions of the dry fallout. Qualitative identification of uranium oxides collected on the substrates of two of the target-area high-volume cascade impactors was also done by X-ray diffraction. The morphologies of selected particles from each of the above three types of samples were studied with a scanning electron microscope and the elemental compositions were determined by microprobe analysis. The details of sample preparation and analytical method are covered in Appendices B.4 and B.5.

3.3.5 Solubility

The solubility of uranium-containing particles in simulated lung fluid was investigated using airborne particulate samples collected in the target area and downwind. Portions of each of the total-particulate sample filters used for uranium oxide determinations were subjected to the solubility analysis. Fractions of the same target-area cascade impactor samples employed in the oxide analyses were also subjected to solubility analysis with the addition of one of the downwind impactor samples. Whereas all five of the substrates from an impactor were used for oxide analysis, only those

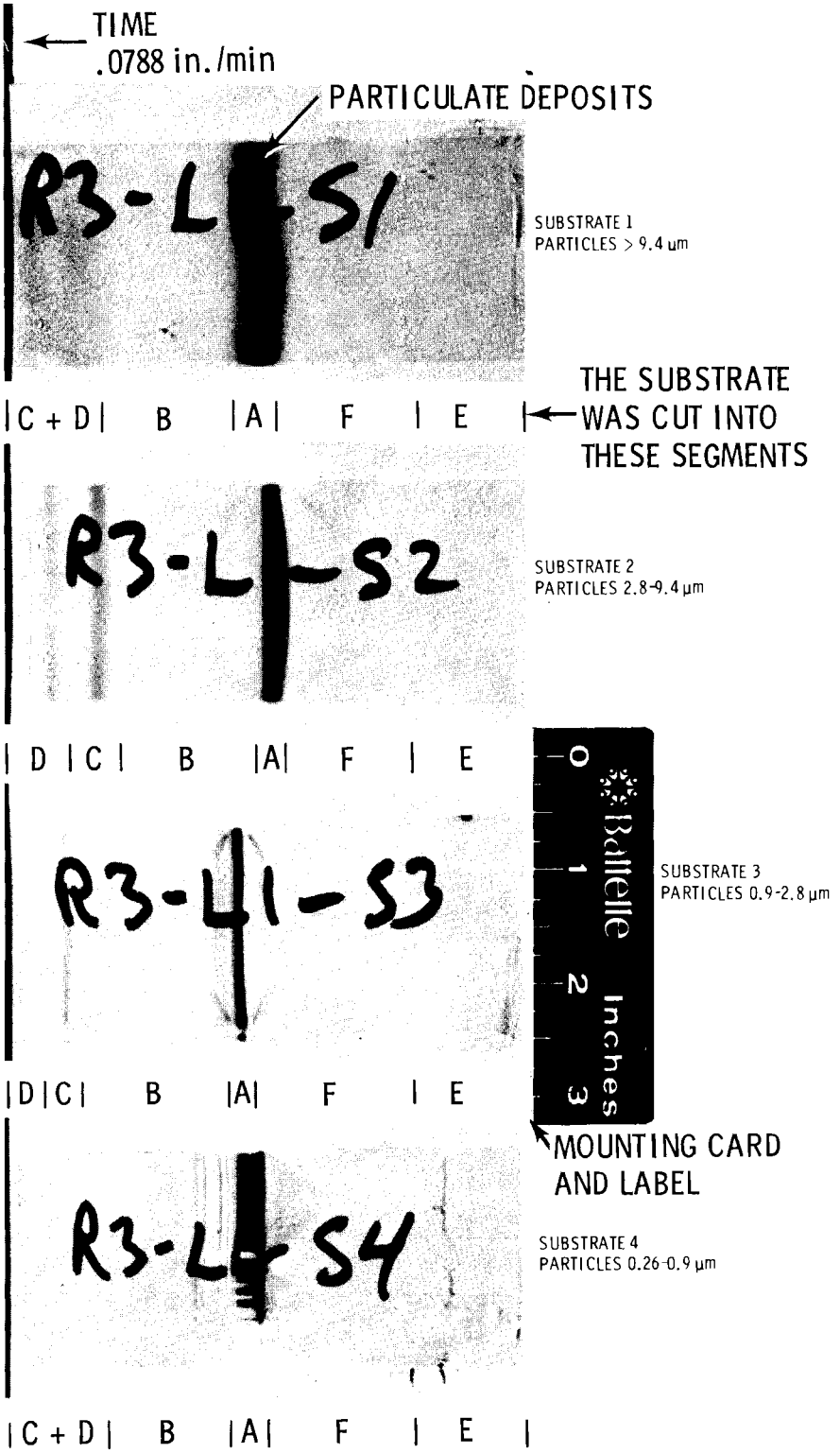

FIGURE 18. Typical Mylar Substrates from Lundgren Impactor

substrates representing respirable particles were used in the solubility analysis. It was reasoned that only respirable particles, approximately 3.3 μm AED or smaller, would penetrate to and be retained in the pulmonary compartment of the lungs. Respirable particles were collected on the last two stages of the impactor and the backup filter (see page 12 and Table 9, page 53).

The solubilities of the materials collected on the samples were measured by immersing them in simulated lung fluid[6] and extracting aliquots at selected times. The aliquots were analyzed for uranium using the fluorometry technique. The starting uranium content of the sample fractions was estimated from analysis of other portions of the same samples. The details of sample preparation and analytical procedure are covered in Appendices B.6 and B.7.

4.0 RESULTS

In this section the results of the experiments and interpretation of the data are summarized. Other detailed data and sample calculations are referenced and included in the appendices.

4.1 AIRBORNE PARTICLE SIZE

4.1.1 High-Volume Cascade Impactors

The size distribution of the airborne uranium is reconstructed from the cascade impactor data by first summing the uranium collected on the stages and backup filter and calculating the percentage of the total mass found on the individual stages. Then, cumulative percentages for each stage are calculated starting with the backup filter and ending with the first stage. An example calculation is shown in Appendix C, Table C.1. The cumulative percent for the backup filter is plotted versus the aerodynamic equivalent cut-off of stage 4 and so on, until the cumulative percent of stage 2 is plotted versus the aerodynamic equivalent cut-off of stage 1. If this is done where the cumulative percent scale is expressed as probability and the particle-size scale is logarithmic, the size distribution frequently approximates a straight line and the aerodynamic particulate sizes are said to be "log-normally distributed." This condition turned out to be the case for all of the high-volume cascade impactor samples except for two of those located up/downwind of the targets. The individual plots are shown in Figure 19. From these plots the cumulative percent of the airborne uranium less than a given aerodynamic size (AED) can be estimated. The particle size corresponding to 50 cumulative percent of the uranium is the mass mean aerodynamic diameter (MMAD). Thus, half the mass of the airborne uranium is associated with particles smaller than the MMAD and half with larger particles. The MMAD and the slope of the line are sufficient to characterize the size distribution.

The analyses of impactor-stage swabs from four samples were not found to be consistent from impactor to impactor. Average fractions (swab ÷ substrate) were calculated for each impactor stage and the resulting corrections applied

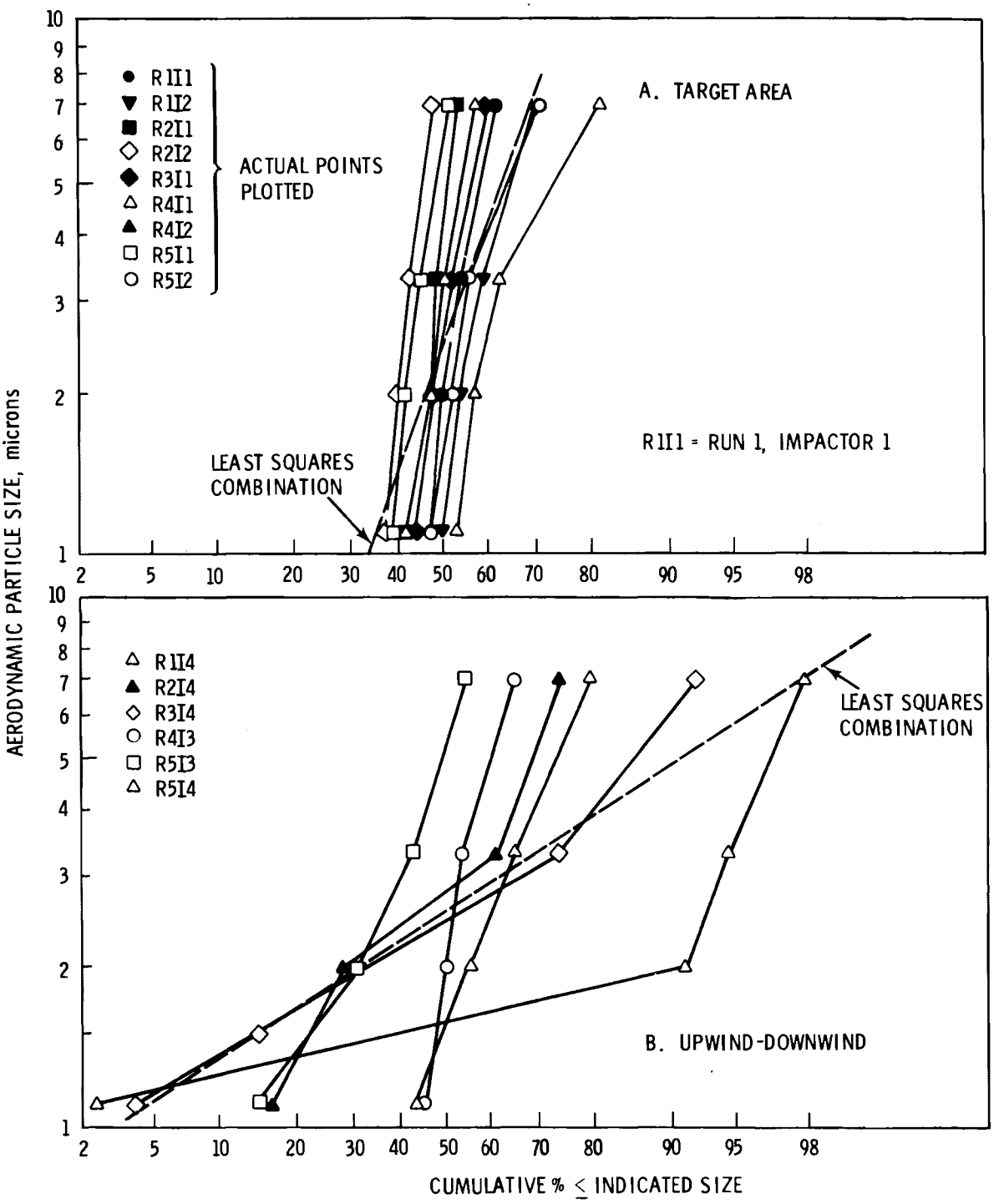

FIGURE 19. Size Distribution Plots for High-Volume Cascade Impactor

to the impactors without swab analyses. The resulting size distributions were neither statistically nor numerically different from those calculated neglecting the swabs. Therefore, the swab analyses were disregarded because of their negligible effect and the uncertainty they would add.

Through the appropriate transformation of each plotted data point shown in Figure 19 least-squares-fitted size distributions were determined and are shown in Figure 20. The target-area size distribution was calculated both with and without the addition of the uranium content of the probe to the content of the first stage. It is reasonable to include the probe with the first stage (cut-off diameter 7 μm), as in Figure 19, for two reasons. First, particle deposition in the pipe is strongly dependent on particle size--the larger the particle the more readily it deposits. Second, one would not expect the MMAD in the target-area to be smaller than downwind from the targets because of the relatively large airborne particles in the impact region that would fall out within a short distance.

Figure 20 shows that the MMADs at the targets were similar to those about 100 ft away. The figure also shows that at the targets the mass percentage of respirable uranium aerosol is smaller than at 100 ft away (56% vs. 70%), indicating large particle fallout over the intervening distance.

It should be pointed out that the size distributions derived from the target-area high-volume impactors carry an uncertainty caused by the clogging of the impactors during the test firings. This is not the case for the up/downwind impactors or the Lundgren impactors (discussed in the following subsection). There was greater variability in the measured MMADs for the target-area impactors than for those up/downwind as shown in Figure 19.

4.1.2 Lundgren Cascade Impactors

The raw data for the Lundgren cascade impactors were reduced as discussed on page 31 and shown in Appendix B.3. The size distribution analysis using the data for the first impactor operating-time interval (which averaged about 5 min) is presented here. The size distributions resulting from the total operating times of the impactors were virtually identical because at least 89% of the airborne uranium measured was collected in the first time interval.

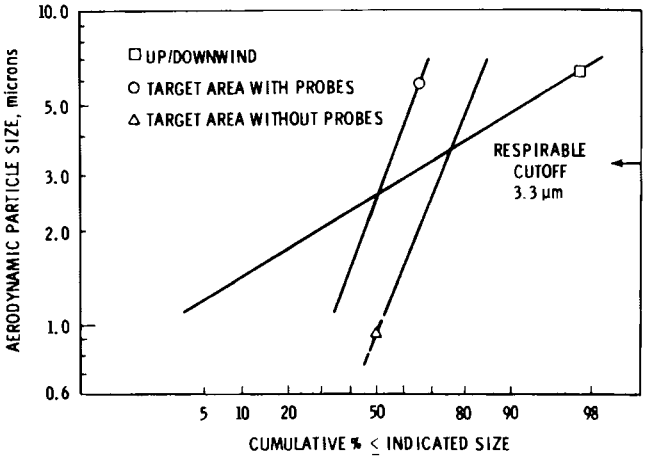

FIGURE 20. Combined High-Volume Impactor Airborne Uranium Size Distributions

The method of deriving size distributions was discussed earlier for the high-volume impactors (page 35) and an example is included in Appendix C, Table C.2.

The size distributions for each impactor sampling from the target accessway are shown in Figure 21 and from behind the X-ray film framework in Figure 22. The corresponding least-squares-fitted lines are also shown in Figures 21 and 22. There is noticeably less variability in these MMADs than in the high-volume impactor data--possibly because these impactors did not clog up.

Figure 23 shows the fitted size distributions from the Lundgren impactors superimposed over those from the high-volume impactors. The similarity of the distributions from the high-volume impactors (probes included) and the accessway Lundgren impactors confirms that uranium aerosol in the target area is coarser[(a)] than at a 110 ft distance from the targets. Both the high-volume impactor (probes excluded) and the Lundgren impactor (behind the framework) distributions show a similar attenuation of large airborne particles by the probes and the framework. Table 4 summarizes the important size distribution data.

(a) Smaller percentage respirable on mass basis.

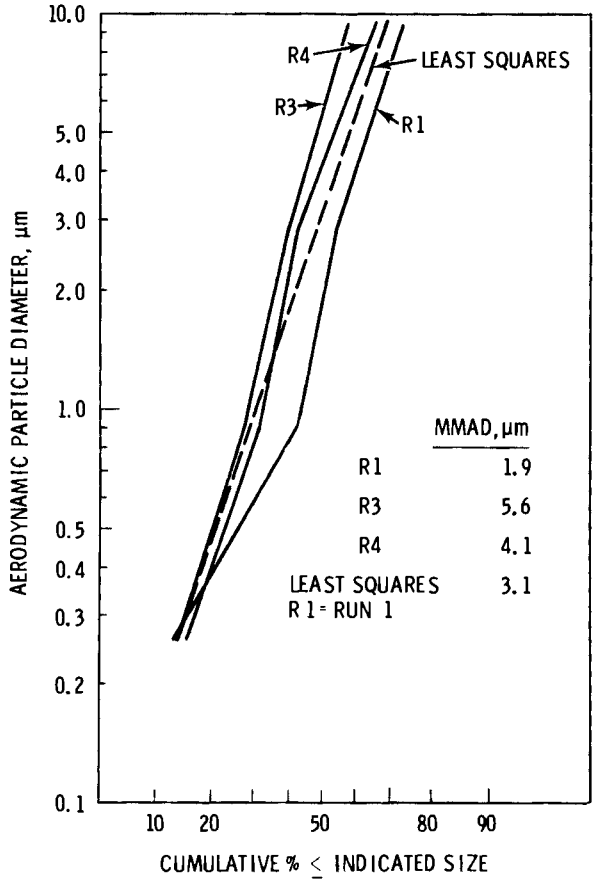

FIGURE 21. Size Distributions for all Lundgren Impactors Sampling from Target Accessway

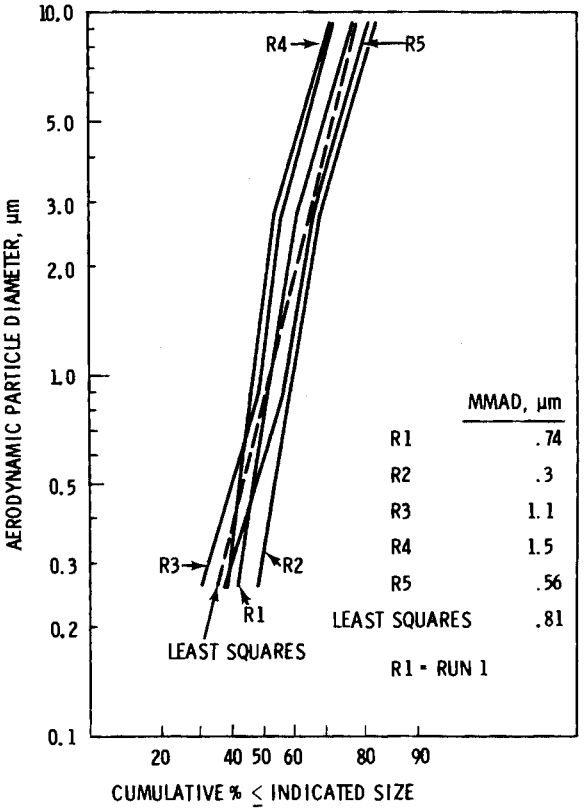

FIGURE 22. Size Distributions for all Lundgren Impactors Behind Film Frame

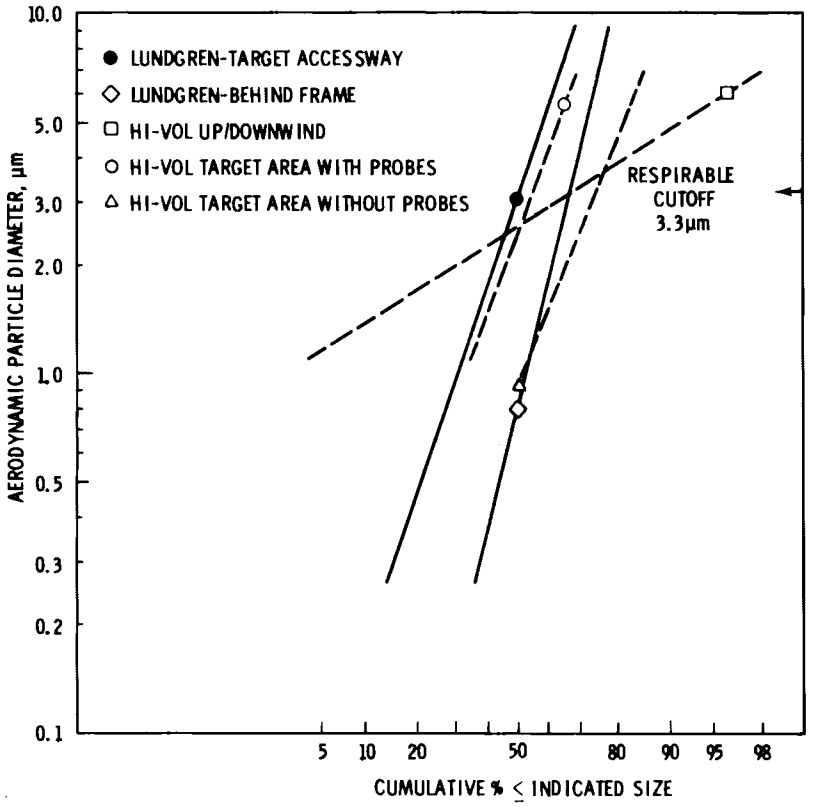

FIGURE 23. Airborne Uranium Size Distributions

TABLE 4. Size Distribution Summary

Impactor	Position	MMAD	% Respirable (≤ 3.3 μm AED)
High-Volume Impactor	Above Targets	2.5	56
High-Volume Impactor	Up/Downwind	2.58	70
Lundgren Impactor	Target Accessway	3.1	51
Lundgren Impactor	Behind Frame	0.81	67

4.2 AIRBORNE URANIUM CONCENTRATION VERSUS TIME

Data from the Lundgren impactor samples were used to estimate the target-area airborne uranium concentration variation with time. The reduction of data to determine the mass of uranium collected over time intervals was described on page 31 and in Appendix B.3. The average airborne uranium

concentration over a time interval was calculated by dividing the mass by the sampler flowrate and time. Examples of these calculations are shown in Appendix D, Table D.1. The resulting concentrations for each time interval are tabulated in Table D.2.

The measured change in airborne depleted uranium concentration with time is summarized in Figure 24. The two envelopes enclose the data points obtained by sampling from the target accessway and behind the X-ray film frame during the usual 15-min post-shot waiting period[a] and usual target-changing activity. The two lines indicate the measured concentrations at the same locations and while no target-changing activity occurred. (This latter condition was studied for only one run). The measured concentrations in the accessway were generally higher than behind the film frame. All measurements were made at breathing level, 5 to 6 ft elevation. Note that the measured concentrations were higher when target changing proceeded as usual than when suspended.[b] The measurements show some increase in concentration as the target-changing activity gets underway. This may be caused by mechanical resuspension of uranium from the soil or other surfaces. For comparison, the maximum permissible concentrations (MPC_a) set in the Code of Federal Regulations[c] for occupational exposure to airborne depleted uranium are noted in the figure for both soluble and insoluble uranium compounds.

4.3 CLOUD VOLUME

The volumes of the clouds generated by the impacts of penetrators were estimated from the tracking films provided by TECOM. To estimate cloud volume, the image of a cloud (at its greatest size and before significant

---

(a) The time interval personnel are required to wait before re-entering the target area.

(b) The sharper drop in concentration during the 15-min waiting period shown by the two lines may be caused by a higher wind speed than experienced during the other runs (2.7 to 5.5 mph versus calm to 3.8 mph).

(c) The MPC_a for insoluble uranium is derived from the value given for natural uranium in 10 CFR 20 using the specific activity of 3.6×10^{-7} Ci/g for depleted uranium. The 10 CFR 20 MPC_a for soluble mixtures of uranium isotopes where the abundance of $^{235}U<5\%$ is used herein.[7]

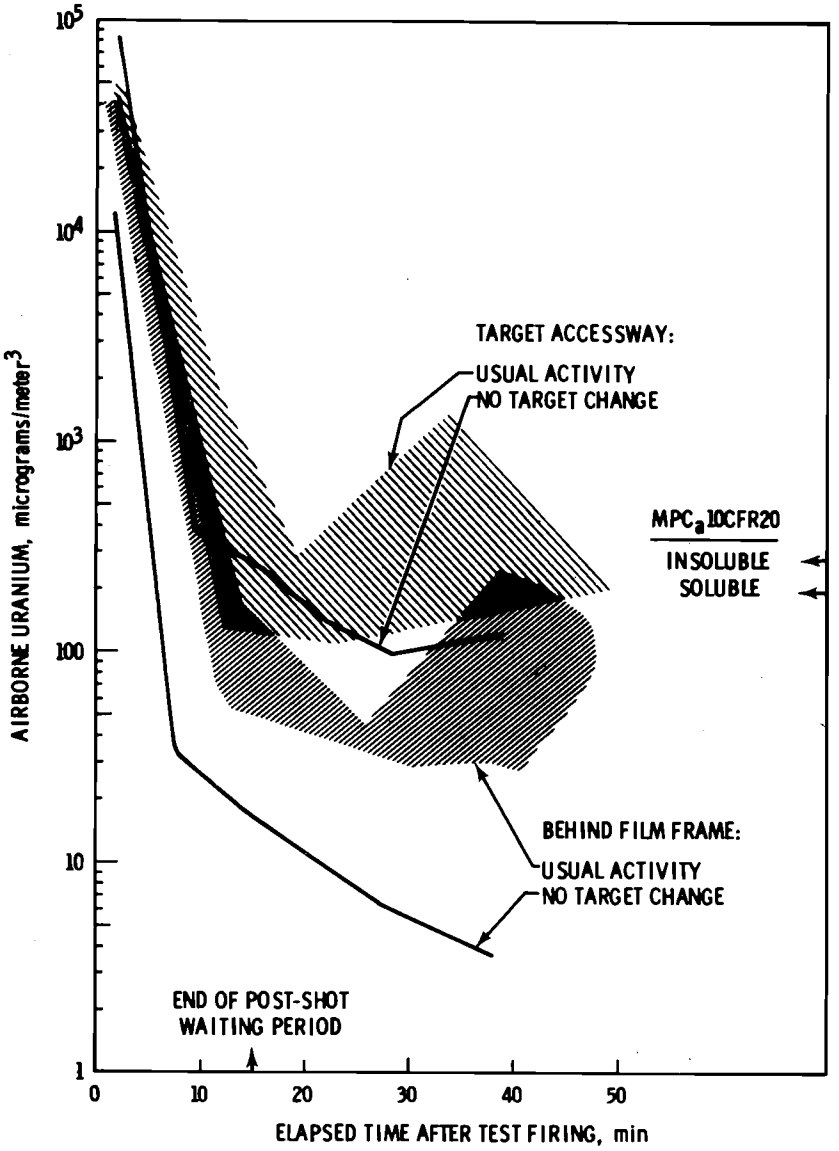

FIGURE 24. Airborne Depleted Uranium Concentration Versus Time

drifting) was projected onto paper, and the cloud and features of the target stand were outlined. A length scale was obtained from features of known dimension. Each cloud outline was divided into units of simple geometric shape (parallelograms and circles) and key dimensions were measured. Volumes were computed assuming the horizontal cross sections were circular. Computations were made for the views of each cloud from two cameras separated by a 57^{o} included angle. Because of the distortion caused by this positioning, a true estimate of depth of each cloud was not possible. The

estimated cloud volumes from the two camera angles were averaged; results are given in Table 5. Both films for Run 5 were overexposed and deleted from the analysis.

TABLE 5. Estimated Cloud Volumes, m^3

Run	Camera No. 22	Camera No. 25	Average Volume
1	1600[a]	1370	1500
2	827	1120	1000
3	556	2750	1700
4	970	2840	1900

(a) Photographic images were slightly overexposed. The value given is a best estimate.

4.4 TOTAL AIRBORNE URANIUM PARTICULATES

The results of the total particulate samples collected in the target area are discussed first and the results for environmental total-particulate samplers follow.

4.4.1 Target-Area Total Airborne Uranium

The total exposure (mass x time/vol) to airborne uranium in the target area was calculated for each run by dividing the total uranium collected by the total volume flowrate of the samplers. Sample calculations are included in Appendix E.

The airborne concentration can be calculated from the total exposure, given the time interval during which the material of interest was sampled. The total mass airborne can then be computed from the cloud volume. Estimating the sampling interval during which the bulk of the airborne material would have passed the probes and estimating the volume of the cloud sampled are the greatest uncertainties in this analysis. The assumption of a homogeneous concentration within the visible cloud and the plugging of samplers add to the uncertainty.

The tracking films of the clouds did not cover a long enough period of time to observe when the visible smoke dissipated from the target area. However, they did show the very rapid growth (10 sec) of the cloud to a very large size. The color movie of Run 4 showed that the most dense cloud moved out of the target area in less than 16 sec (the view of the camera was changed to follow the smoke as it drifted across the range.) The width of the initial deposits on the Lundgren impactor substrates indicates that the deposits were collected in less than a minute although the substrate rotation speed was not fast enough to resolve the time any finer than that.

It would not be reasonable to assume that the total-particulate samplers operated at full flow and instantly plugged when the cloud dispersed from the target area. From examination of the color movie from Run 4 and the Lundgren impactor substrates, the samplers probably plugged in less than 15 sec after the shot. The study has assumed, then, that the samplers operated at full flow for 5 sec and that the flow decreased linearly to zero at 10 sec, which is equivalent to assuming a sampling interval of 7.5 sec at 50 cfm for each sampler. The calculated airborne uranium concentration and mass for each run are shown in Table 6 based on these assumptions. The average fraction of the penetrator as airborne particulates was 70%. This result, however, suffers from the uncertainties mentioned in this subsection and from the likelihood that some of the particulates sampled are resuspended from the soil and target stand. It cannot be stated conclusively how much of the respirable particulates came from the penetrator impact or from material resuspended by the concussion. Of the roughly 2.4 kg of airborne depleted uranium generated during a test firing, about half of that is respirable particulates based on the size distribution discussed earlier (see Table 4).

4.4.2 Environmental Airborne Uranium

The analysis of environmental airborne uranium was based on the total particulate (T7, T8) and cascade impactor (I3, I4) samples collected at a distance of 80 to 150 ft from the target, and the total particulate samples

TABLE 6. Total Airborne Uranium Assuming 7.5 sec Sampling Interval at 50 cfm

Run	Exposure mg min/m^3	Concentration[a] mg/m^3	Cloud[b] m^3	Airborne[c] g	Approximate Mass % of a Penetrator[d]
1	150	1200	1500	1800	53
2	153	1220	1000	1220	36
3	215	1720	1700	2924	87
4	231	1850	1900	3515	104
				9,459	
				Ave = 2,365 or	70%

(a) Concentration $= \left[\frac{mg \times min}{m^3}\right] \times \left[\frac{1}{0.125\ min}\right]$

(b) From Table 5.

(c) g = cloud, $m^3 \times \frac{mg}{m^3} \times \frac{g}{1000\ mg}$

(d) $\frac{c}{3365\ g} \times 100$

collected outside the Ford's Farm Firing Range. These offsite samples were collected at the Human Engineering Lab (HEL) field, Mile Test Loop (MTL) and Building 938 at Michaelsville as shown in Figure 10. Most of the samples from the Staplex samplers at Ford's Farm were not analyzed because of cost factors. Airborne uranium concentration was calculated by dividing the mass of uranium collected by the flow rate and collection time. For the samplers at Ford's Farm, the assumed collection time was the elapsed time the samplers operated after the shot was fired. For the samplers at HEL and MTL, the actual operating time was used for the calculations.

Table 7 summarizes the concentration at each location and indicates whether the sampler was located downwind, upwind or crosswind. It was not always known for certain whether the HEL and MTL samplers were downwind or upwind because the wind direction varied considerably as shown in Appendix A.2.

TABLE 7. Environmental Airborne Uranium Concentrations

Run/Firing Time	Approximate Orientation of Sampler	Operating Time, min	Concentration $\mu g/m^3$
1/1803	T8 Downwind	20	16
	I4 Downwind	20	690
	S4 Downwind	20	8.9
	S3 Downwind	20	5.8
	T7 Upwind	20	12
	MTL Crosswind	446	0.44
2/0951	I4 Crosswind	15	82
	MTL Crosswind	112	0.14
3/1722	T8 Downwind	16	1.8
	I4 Downwind	16	110
	HEL Crosswind	180	0.091
	T7 Upwind	16	4.5
4/1401	T7 Downwind	94	39
& 1508	I3 Downwind	94	93
	MTL Downwind	287	0.045
	HEL Downwind	346	0.053
	T8 Upwind	94	0.40
5/0850	T7 Crosswind	19	4.5
	I3 Crosswind	19	80
	T8 Downwind	19	100
	I4 Downwind	19	250
	MTL Upwind	395	0.022
	HEL Upwind	309	0.046
Oct. 7-8[a]	Bldg 938	1270	0.43
Oct. 7-8[a]	Michaelsville	1293	0.41

(a) During Runs 4 and 5.

The table also includes the concentration measured by the Army at Building 938 and Michaelsville with routine environmental samplers (see Figure 10).[a]

Table 7 shows that the concentrations at the locations distant from Ford's Farm (see Figure 10) were lower than at the range and well below the MPC_a for nonoccupational exposures set at 7 $\mu g/m^3$ for soluble airborne particles and 10 $\mu g/m^3$ for insoluble.[6] The agreement between adjacent pairs of samplers at Ford's Farm--T7, I3, and T8, 14--was not good. These adjacent samplers were only as far as 15 ft apart. It is possible that one and not the other adjacent sampler caught the edge of the plume although the impactors always gave higher readings. Some Ford's Farm downwind concentrations exceeded the occupational MPC.

4.5 FALLOUT

The quantities collected during the wet and dry fallout experiments and the mass associated with a few fragments of depleted uranium are discussed in this subsection.

4.5.1 Wet Fallout

The estimated amount of fallout collected in each sector shown in Figure 16 was calculated by multiplying the quantity found in each tray by the sector area and dividing by the area of the tray. Figure 25 shows the estimated quantity of uranium in each sector.

The total quantity estimated within 50 ft of the target center for six test firings is 2157 g uranium or 359 g per test firing. Therefore, about 11% of a penetrator could be accounted for on the ground or structures within a 50-ft radius; however, some fallout collected may have been resuspended ground contamination. The amount of fallout in the immediate target vicinity was probably underestimated as a result of the fact that no fallout tray was

---

(a) In this case, the samples were alpha-counted by the Army and the result reported as $\mu Ci/m^3$. The concentration in Table 7 assumes this was all depleted uranium.

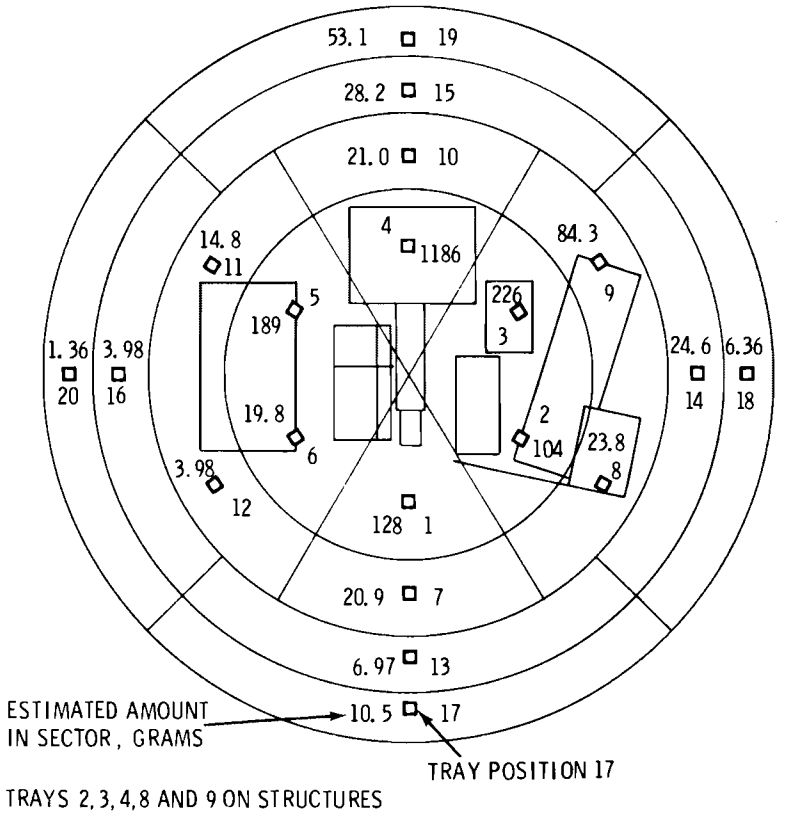

FIGURE 25. Estimated Amount of Uranium Fallout in Sectors Within 50 ft of Target Center

closer than 10 ft to the targets. Using a figure of 360 g per firing, 36 kg of depleted uranium would be deposited with a 50-ft radius (730 m^2) after 100 firings. This estimate does not include the larger fragments discussed later. Also, there is likely to be some fallout outside the 50-ft radius as well.

4.5.2 Dry Fallout

The dry fallout trays collected material from nine test firings, a total of 169 g of fallout, dirt and wood chips. Small samples of the collected

materials were submitted for uranium analysis. The collected fallout material contained 19% uranium by weight. These samples were collected mainly for the identification of uranium oxides as detailed later.

4.5.3 Fragments

Over months, large fragments of penetrators have been collected during the test firing program. These large fragments were picked up and stored in a container near the catcher. Undoubtedly, many fragments were not picked up. Most of the large fragments are identifiable as being from the tail section of the penetrator.

Two large fragments, some smaller ones and some powder were picked up off the ground and selected from the fragment storage container. The fragments were irregular in shape and gray in color with a greenish-yellow tinge. Polished metal surfaces were evident from the machining operations. The machined "flutes" of the penetrator were easily recognized on the two largest fragments. These two fragments weighed 124 and 194 g each (3.7% and 5.8% of a 3.365 kg penetrator).

4.6 URANIUM OXIDES

Uranium is a pyrophoric metal and, at elevated temperatures, can ignite and oxidize rapidly.[7,8,9,10] Four uranium oxides have been established--UO_2, U_4O_9, U_3O_8, and UO_3--plus a large number of non-stoichiometric uranium-oxygen combinations.[12] The most commonly encountered oxides are UO_2 (which by X-ray diffraction pattern must be considered UO_{2+x} where x is less than 0.33) and U_3O_8. For the test firing conditions, it was anticipated that all the depleted uranium made airborne would be in the form of oxides.

Inhalation and deposition of uranium oxides in the deep lung can pose two hazards. If the material is insoluble, the lung tissue is subjected to internal irradiation. If the material is soluble, the chemical toxicity affects the kidneys.[13] Uranium is soluble in body fluids (interstitial lung fluid, blood serum, etc.); the rate at which uranium goes into solution

depends upon its starting oxidation state and surface area.[14] Thus, knowledge of the solubility of the airborne material is important in deciding which limitation to impose--that based upon irradiation or chemical toxicity.

Identification and relative abundance of uranium oxides present in selected samples of airborne material collected over the targets during test firings and in dry fallout material was performed by comparison with American Society for Testing Materials diffraction patterns for these compounds and integration of the area of the identifying peaks. Elemental analysis by X-ray fluorescence micro-probe were also performed to determine the amount of other material that might be involved with the airborne depleted uranium. Photomicrographs using a scanning electron microscope (SEM) were obtained as part of the particle selection process for the elemental analysis and are presented as an indication of the morphology of the airborne particles.

4.6.1 Total Particulate Samples

The relative abundance of UO_2:U_3O_8 in the airborne material collected over the target during each firing was determined from the total particulate sample with the highest measured uranium mass from each run. The estimated relative abundances determined are listed in Table 8. The crystalline phase in all the samples appears to be a relatively homogeneous mixture of UO_2 and U_3O_8 and elemental analysis of individual particles indicates 1% to 5% by weight of iron and tungsten are present.

TABLE 8. Relative Abundance of Uranium Oxides in Target Area Samples

Run Sample	UO_2 Weight Percent	U_3O_8 Weight Percent
1-T2	25	75
2-T1	28	72
3-T2	30	70
4-T3	27	73
5-T2	29	71

Figure 26 shows photomicrographs of individual particles at two magnifications--1200 X and 3000 X. At 3000 X, the particles appear to be roughly spherical and composed of many small particles ranging from 0.03 to 0.1 m in diameter.

4.6.2 High-Volume Cascade Impactor Samples

The oxide forms present in various size fractions of airborne material collected over the target were determined for two runs (3 and 4). The mass of material was insufficient for a quantitative estimate, but the oxides are listed in the order of estimated abundance in Table 9. Analysis of individual particles indicates that the principal constituents are uranium and iron with minor quantities of tungsten, aluminum, and silicon. The ratios of uranium to iron are also listed in Table 9 and range from 5:1 to 13:1 with the ratio increasing with decreasing size (20% to 8% iron). Much higher U:Fe ratios (100:1 to 20:1) were observed for the total particulate samples. A possible explanation is the loss of a portion of smaller particles during the high air-velocity flow (when the particle concentrations are highest) as a result of non-isokinetic sampler flow.

Most of the particles examined using the scanning election microscope were dark spheres, but some samples also contained amorphous particles ranging from yellow to reddish orange. Analysis indicates that their major constituents are iron and tungsten with essentially no uranium. Figure 27 consists of photomicrographs at various magnifications of the material found on the stages and backup filter of high-volume cascade impactor I2 during Run 3.

4.6.3 Dry Fallout Samples

Uranium dioxide was the predominant uranium compound observed in the dry fallout material analyzed with only trace quantities of U_3O_8 found. Analysis of individual particles showed uranium to be the principal cation present with some silicon, iron, and tungsten. Figure 28 shows photomicrographs of individual particles observed at two magnifications and indicates the coarse nature of the material.

a. Showing some spherical particles
1200 X.

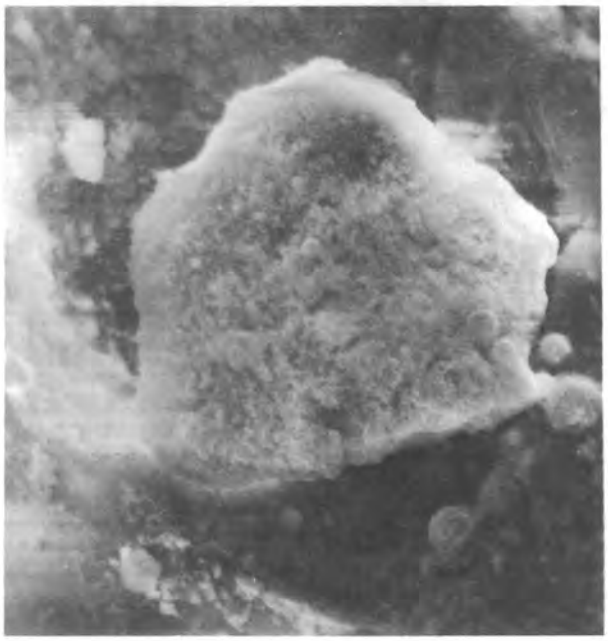

b. This particle is made of fine
crystalline uranium oxides
3000 X.

FIGURE 26. Scanning Electron Micrographs of Particles Collected on Filter Paper

TABLE 9. Characteristics of Material Collected in a Target Area High-Volume Cascade Impactor During Runs 3 and 4

	Size Range μm	U:Fe wt ratio[a]	U Compounds Identified[b]
Run 3-I2	>7.0	5.4 ± 0.4	UO_2, U_3O_8
	3.3 to 7.0	9.6 ± 9.7	UO_2, U_3O_8
	2.0 to 3.3	8.7 ± 0.5	UO_2, U_3O_8
	1.1 to 2.0	7.8 ± 0.4	UO_2, U_3O_8
	<1.1	12.8 ± 0.4	U_3O_8
Run I2	>7.0	5.2 ± 0.6	UO_2, U_3O_8
	3.3 to 7.0	6.0 ± 0.7	UO_2, U_3O_8
	2.0 to 3.3	6.6 ± 0.5	UO_2, U_3O_8
	1.1 to 2.0	8.2 ± 0.2	UO_2, U_3O_8
	<1.1	12.8 ± 0.4	U_3O_8, UO_2

(a) Average of four measurements ± standard deviation.
(b) The compounds are listed in order of estimated abundance.

4.7 SOLUBILITY

The solubility in simulated lung fluid of airborne depleted uranium collected over the target during these test firings was measured for eight specimens. The eight specimens were the total particulate sample from each run containing the highest mass of uranium plus the "respirable fraction" (last two stages and backup filter) from one high-volume cascade impactor from Run 3 and two high volume cascade impactors from Run 4. The samples from the cascade impactors were included to ascertain if a difference in solubilities existed for the finer size fraction. Impactor Run 4-I3 was not in the target area (as were the other two impactors) but in a "downwind" location (see Figure 19). The experimentally measured solubilities are summarized in

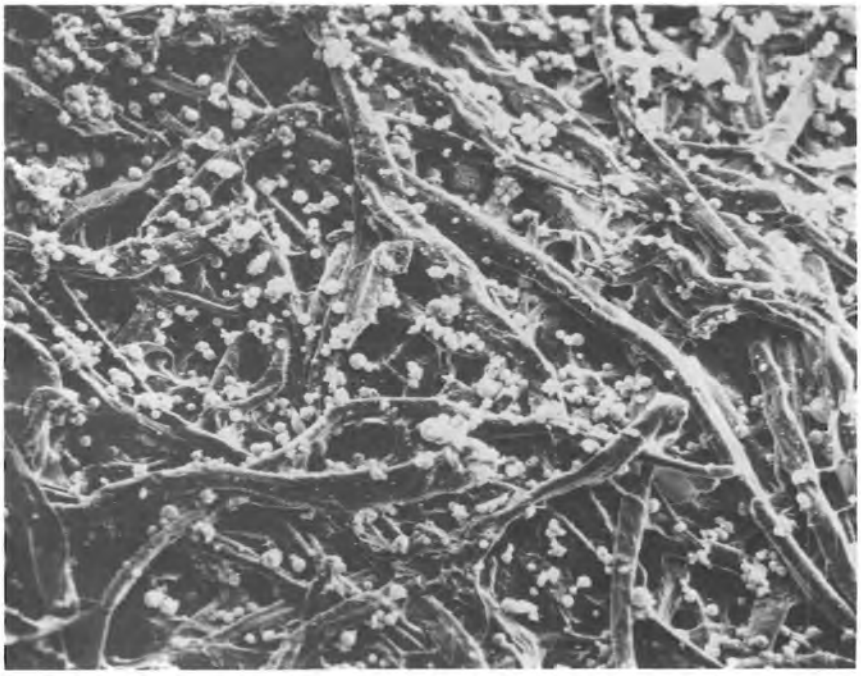

a. Stage 1, 200 X magnification

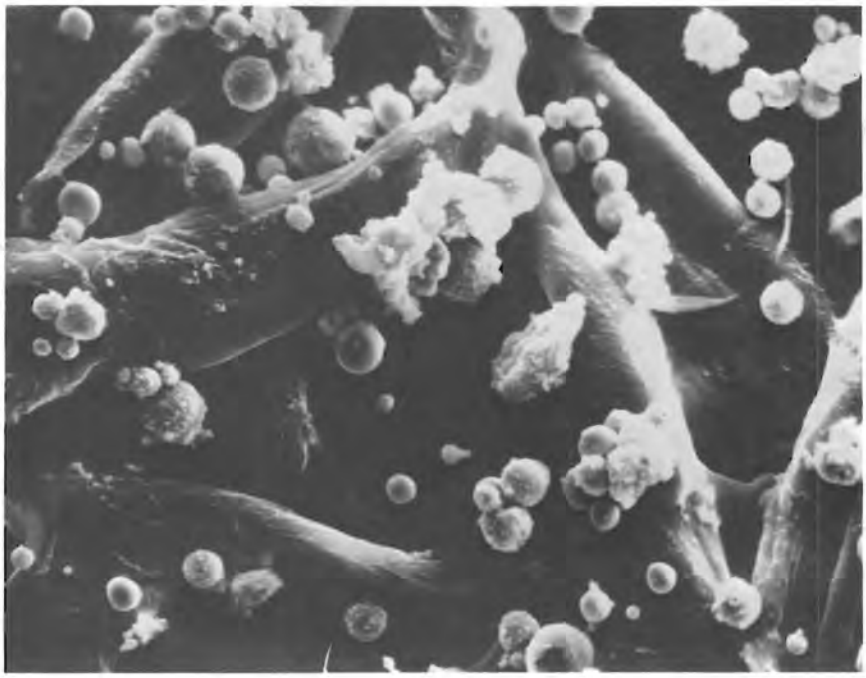

b. Stage 1, 1000 X magnification

FIGURE 27. Scanning Electron Microscope (SEM) Photomicrographs of Materials Collected in a Target Area High-Volume Cascade Impactor During Run 3

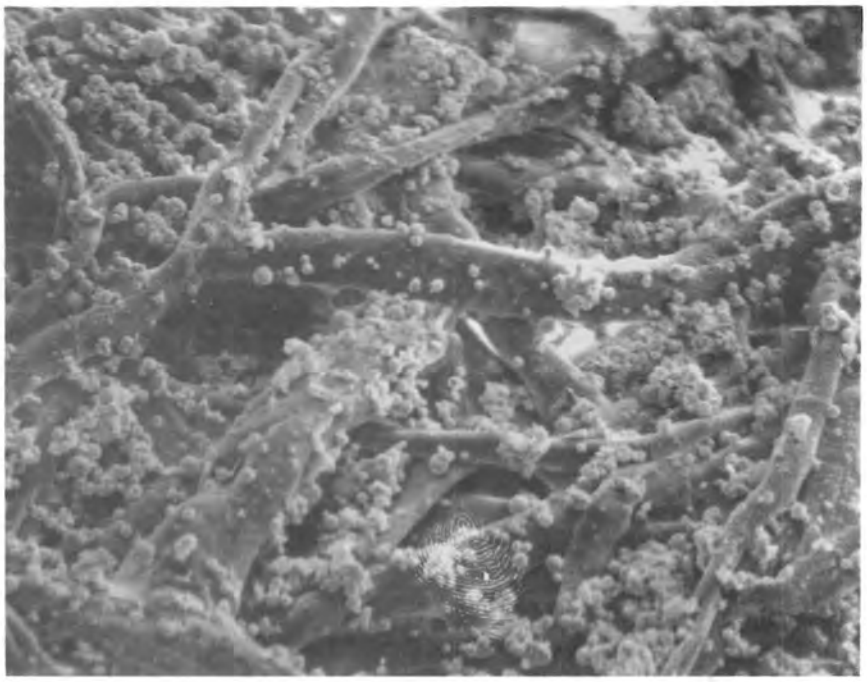

c. Stage 2, 500 X magnification

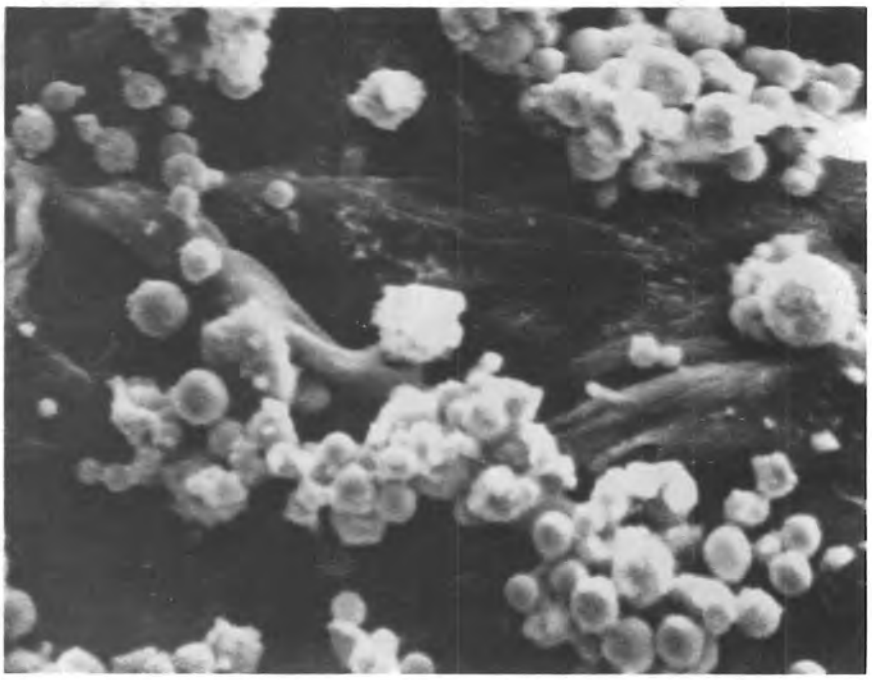

d. Stage 2, 2000 X magnification

FIGURE 27. SEM Photomicrographs of Materials Collected in a Target Area High-Volume Cascade Impactor During Run 3 (contd.)

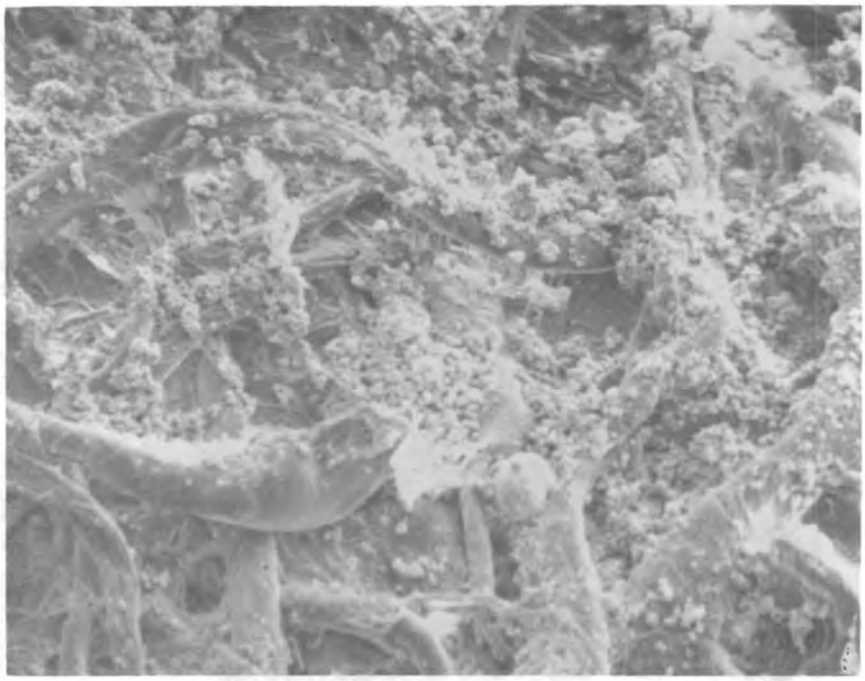

e. Stage 3, 500 X magnification

f. Stage 3, 2000 X magnification

FIGURE 27. SEM Photomicrographs of Materials Collected in a Target Area High-Volume Cascade Impactor During Run 3 (contd.)

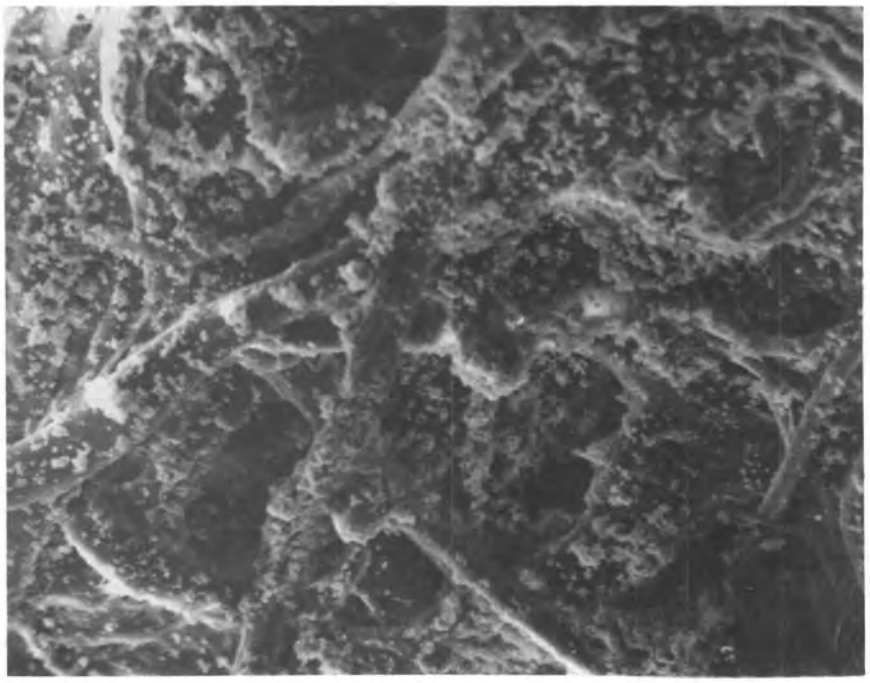

g. Stage 4, 500 X magnification

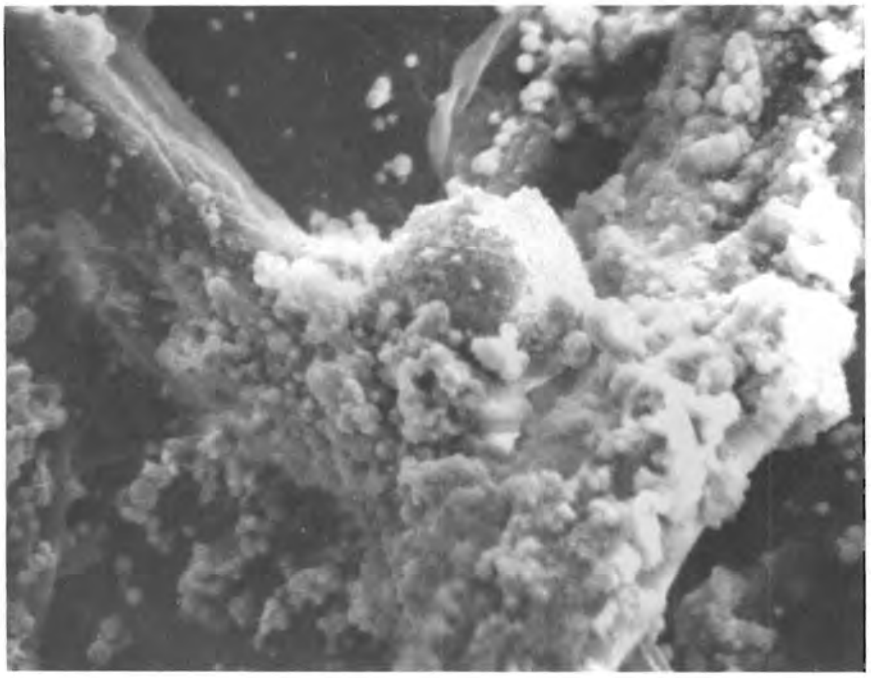

h. Stage 4, 2000 X magnification

FIGURE 27. SEM Photomicrographs of Materials Collected in a Target Area High-Volume Cascade Impactor During Run 3 (contd.)

i. Backup filter 200 X magnification

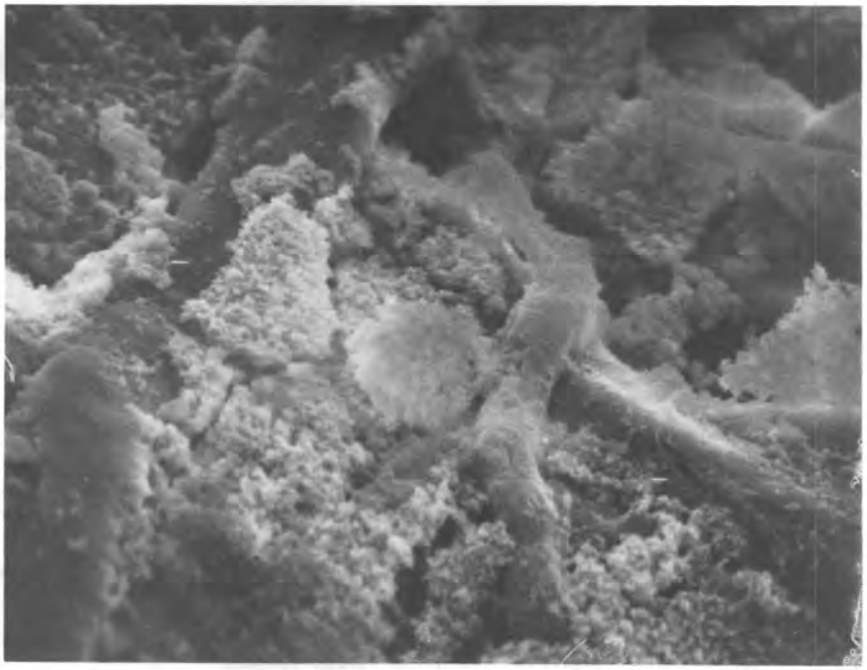

j. Backup filter 1000 X magnification

FIGURE 27. SEM Photomicrographs of Materials Collected in a Target Area High-Volume Cascade Impactor During Run 3

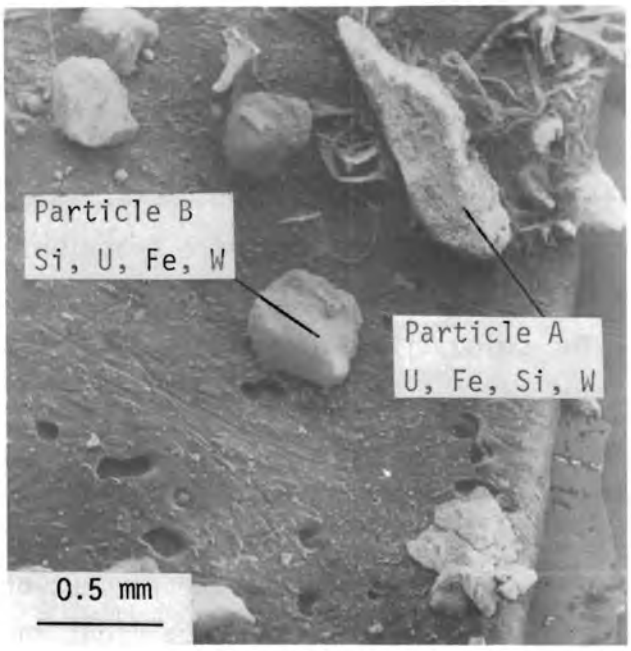

a. Showing particle distribution and chemical compositions

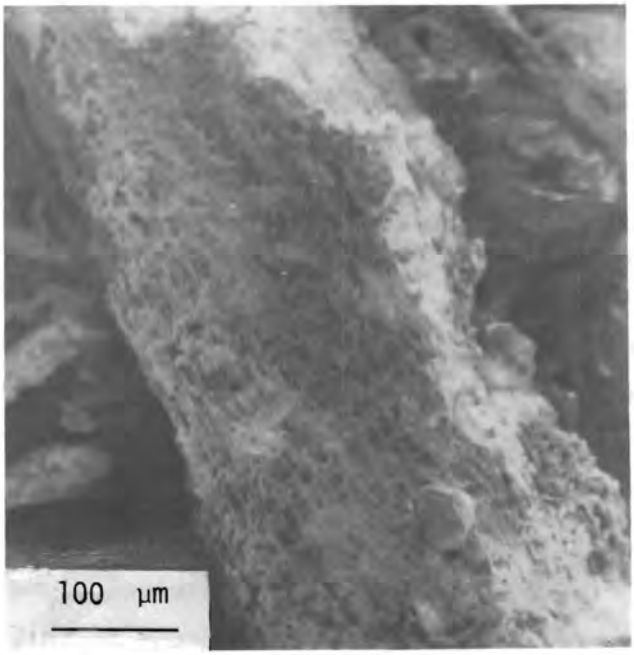

b. Enlargement of Particle A showing some spherical particles and fine crystalline uranium oxide

FIGURE 28. Scanning Electron Micrographs of Sample Fallout

Table 10. The table shows that some uranium is soluble within the first week and that the remainder is essentially insoluble.

The 7-day apparent solubility of the uranium in the finer size fraction averaged 43% (see Table 10, respirable samples) and is two to three times greater than the airborne depleted uranium collected in the total particulate samplers. Table 9 appears to indicate that the fraction of U_3O_8 increases with decreasing size (only U_3O_8 was found in the smallest size fraction in impactor Run 4-I3). The solubility of U_3O_8 in carbonate solution (e.g., lung fluid, etc.) is 700 µg/ml. The difference in solubility cannot be explained completely by the difference in solubility of U_3O_8 and UO_2. Even if UO_2 is considered insoluble, from 26% to 35% of the material on the total particulate sample should dissolve in 7 days since they are $\sim$3/4 U_3O_8 (see Table 8). Figure 29 is a plot of the percent of material dissolved in 7 days versus the mass of uranium present in the sample and indicates solubility may be influenced by the mass packing of material on the filter sample. Another possible explanation for the decrease of solubility of the material collected on the total particulate samples may be the presence of extraneous material coating some of the particles or inhibiting the dissolution of part of the uranium.

4.8 DOWNWIND DOSE

It was the intent of the study to provide some examples of downwind dose calculations to illustrate the influence of distance and stability class. The calculations were made but the measured solubilities for the airborne depleted uranium in the respirable fraction indicated a significant toxicological hazard that was not within the scope of this project. Providing a calculational methodology to indicate the potential radiological hazard without providing a means of assessing the damage as a result of chemical toxicity might lead to the inference that radiological hazard is more significant. Such a decision is beyond the scope of this project and has not been investigated. The example calculations are not included so as to not mislead the reader but are available.

TABLE 10. Measured Solubilities of Airborne Depleted Uranium in Simulated Lung Fluid

Run Sample	Percent of Uranium into Solution in 7 Days	Approximate Dissolution Rate after 7 Days, (Percent Extracted per Day (a,c)
Run 3-I2(b)	47 + 10	0.1 + 0.7
Run 4-I2(b)	34 + 8.0	-0.5 + 0.5
Run 4-I3(b)	49 + 14	-0.5 + 1.0
Run 1-T2	16 + 3	0.2 + 0.2
Run 2-T1	13 + 3	-0.05 + 0.2
Run 3-T2	18 + 4	0.05 + 0.3
Run 4-T3	11 + 3	0.01 + 0.2
Run 5-T2	15 + 4	0.05 + 0.3

(a) A negative value indicates uranium lost or reabsorbed.
(b) Respirable fraction only.
(c) ± Estimated Standard Error

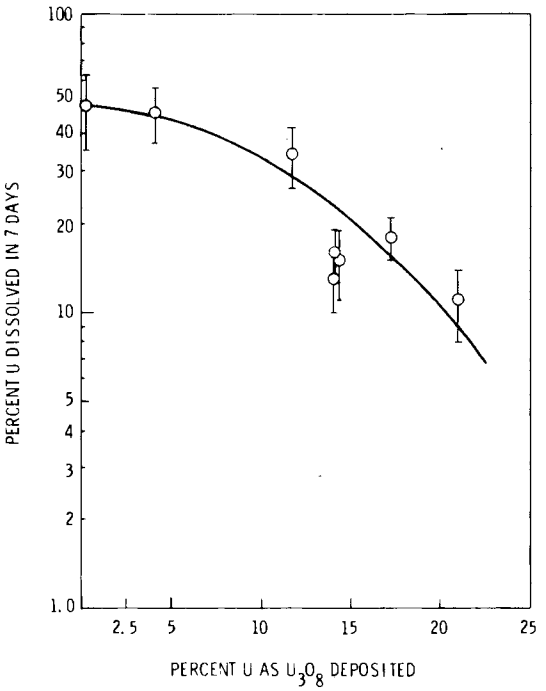

FIGURE 29. Percent Uranium Soluble in Seven Days Versus Mass of Uranium (as U_3O_8) in Sample

5.0 REFERENCES

1. R. L. Gilchrist, G. B. Parker and J. Mishima, Radiological and Toxicological Assessment of an External Heat (Burn) Test of the 105 mm Cartridge, APFSDS-T, XM-774. PNL-2670, Pacific Northwest Laboratory, Richland, WA 99352, March 1978.

2. R. L. Gilchrist, W. T. Bartlett and G. W. R. Endres, Radiation Dose Rate Measurements Associated With the Use and Storage of XM-774 Ammunition. PNL-2947, Pacific Northwest Laboratory, Richland, WA 99352, 1979.

3. W. C. Hanson, J. C. Elder, H. J. Ettinger, L. W. Hantel and J. W. Owens, Particle Size Distribution of Fragments from Depleted Uranium Penetrators Fired Against Armor Plate Targets. LA-5654, Los Alamos Scientific Laboratory, Los Alamos, NM, October 1974.

4 Thomas T. Mercer, Aerosol Technology in Hazard Evaluation. Academic Press, New York, NY, pp. 287-293, 1973.

5. F. A. Gifford, "Turbulent Diffusion - Typing Schemes: A Review," Consequences of Effluent Release. R. L. Shoup, ed., Nuclear Safety. 17, 68-76, Jan.-Feb. 1976.

6. O. R. Moss, "Simulants of Lung Interstitial Fluid." Health Phys., 36, 447-448, 1979.

7. Code of Federal Regulations. Title 10, chapter 1, part 20, appendix B. Superintendent of Documents, U.S. Government Printing Office, Washington DC, pp. 168-169, January 1977.

8. E. M. Mouradian and L. Baker, Jr., "Burning Temperatures of Uranium and Zirconium in Air." Nuclear Science and Engineering. 15:388-394, 1963.

9. L. Leibowitz, L. Baker, Jr., J. G. Schnizlein, L. W. Mishler and J. D. Bingle, "Burning Velocities of Uranium and Zirconium in Air." Nuclear Science and Engineering. 15:395-403, 1963.

10. L. Baker, Jr., J. G. Schnizlein and J. D. Bingle, "The Ignition of Uranium." Journal of Nuclear Materials. 20:22-38, 1966.

11. L. E. Musgrave, "A Theory of Burning Curve Ignition of Nuclear Metals." Journal of Nuclear Materials. 43:155-163, 1972.

12. H. C. Hodges, J. N. Stannard and J. B. Hursh, eds., Uranium, Plutonium, Transplutonium Elements. Springer-Verlag, New York, 1973.

13. E. J. Bennellicke, A Review of the Toxicology and Potential Hazards of Natural, Depleted, and Enriched Uranium. AHSB-RP-R58, Authority Health and Safety Branch, United Kingdom Atomic Energy Authority, U.K., 1966.

14. H. B. Wilson, H. E. Stockinger and G. E. Sylvester, "Acute Toxicity of Carnolite Ore Dust." Archives of Industrial Health. 7:301-309, April 1953.

APPENDIX A.1

PLACEMENT AND OPERATION OF SAMPLERS

RUN 1--OCTOBER 4, 1977, ROUND FIRED 1803

When the samplers were shut-off, the flowmeters of target-area samplers T1-T6, I1, and I2 read below scale. The other air samplers were operating as set except that T7 read 35 cfm and I3 read about 22 cfm.

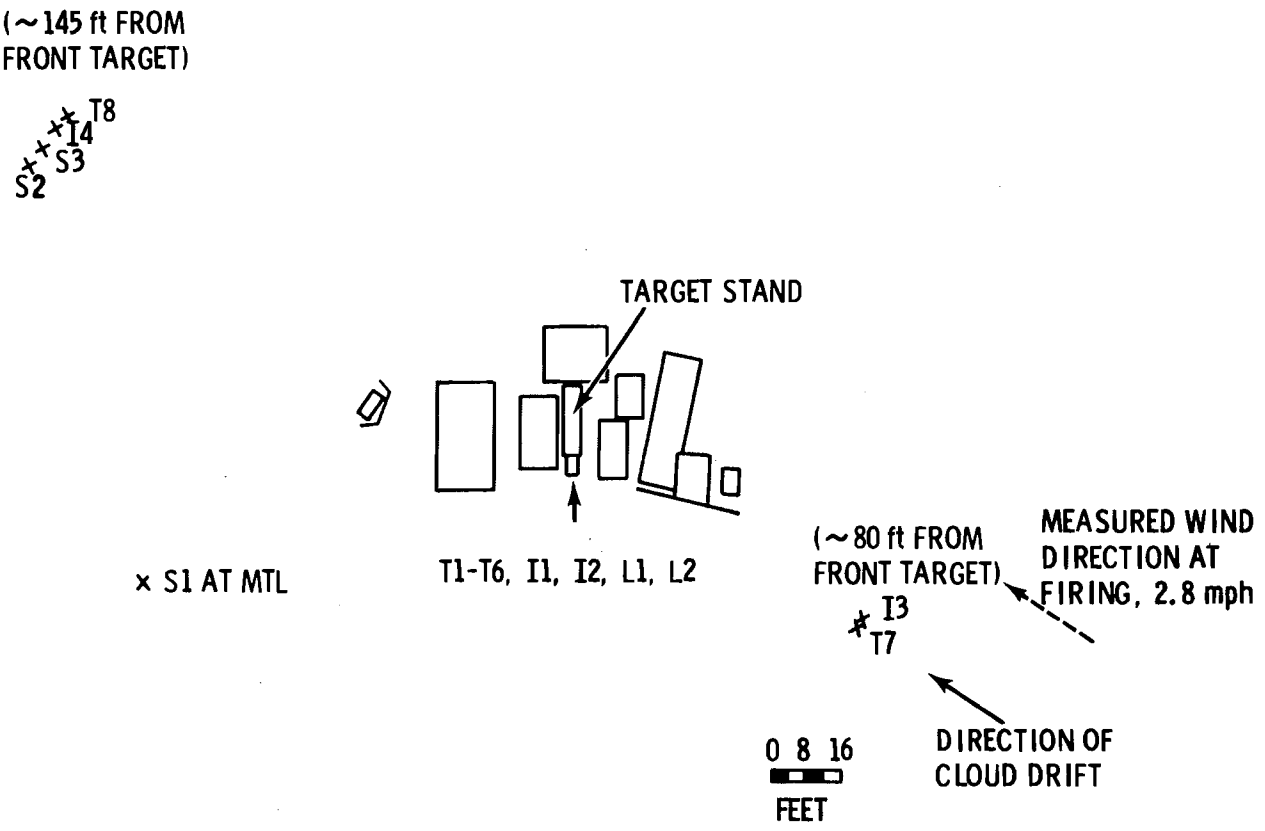

FIGURE A.1.1. Sampler Placement Run 1, October 4, 1977

TABLE A.1.1. Sampler Operation, Run 1, October 4, 1977

Sampler	Time on	Time off	Duration (min)	Assumed Average Flowrate, cfm
T1-T6[a]	1758	1823	?[e]	50
T7	1758	1823	25	42
T8	1758	1823	25	50
I1,[b] I2	1758	1823	?	20
I3, I4	1758	1823	25	20
L1, L2[c]	1758	1852	54	3
S2	1758	1823	25	26
S3	1758	1823	25	26
S1[d]	1217	1517	446	25
S1	1519	1945		

(a) T6: Total Particulate Sampler #6.
(b) I1: High-Volume Cascade Impactor #1.
(c) L2: Lundgren Impactor #2.
(d) S1: Staplex Sampler #1.
(e) Time not accurately known due to sampler clogging or other malfunction

RUN 2--OCTOBER 6, 1977, ROUND FIRED 0951

This run was performed during a light rain. The fuse burned out on impactor L1, and the impactor was removed from the area. Power to the upwind samplers was lost, probably because the addition of sampler S5 overloaded the circuit. The cloud formed into a mushroom shape, rose about 100 to 150 ft, and drifted over the trees east of the target, missing the downwind samplers.

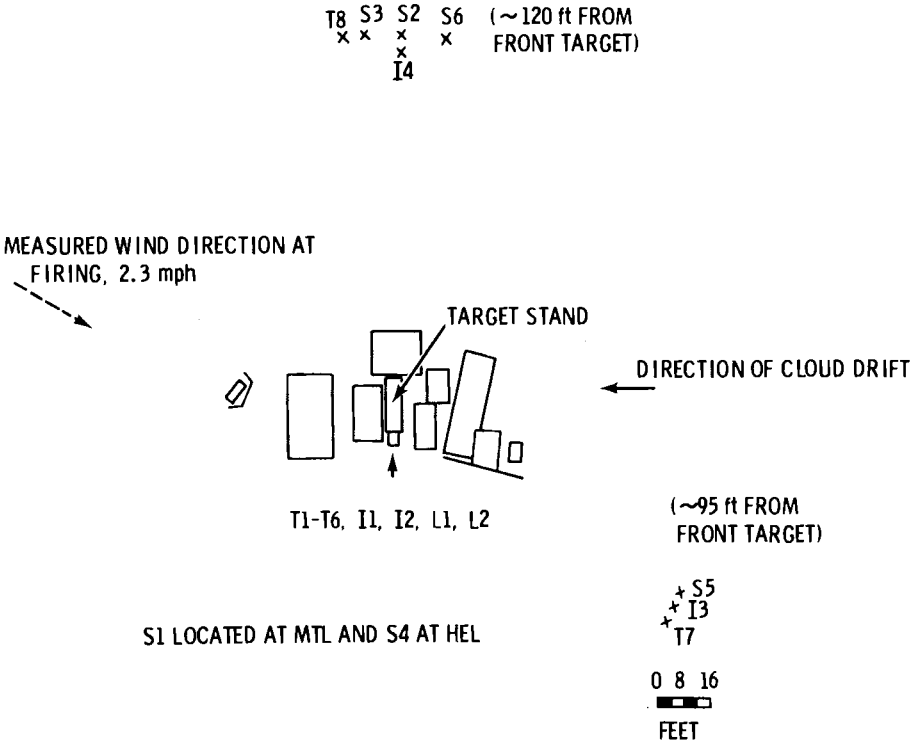

FIGURE A.1.2. Sampler Placement Run 2, October 6, 1977

TABLE A.1.2. Sampler Operation, Run 2, October 6, 1977

Sampler	Time on	Time off	Duration (min)	Assumed Average Flowrate, cfm
T1-T6	0940	1006	?	50
T8	0940	1006	?	?
I1, I2	0940	1006	?	20
I4	0940	1006	26	20
L2	0940	1010	30	3
S1	0823	1015	112	25
S2	0940	1006	26	26
S3	0940	1006	26	26
S4	0750	?	?	24
S6	0940	1006	26	35

RUN 3--OCTOBER 6, 1977, ROUND FIRED 1722

At startup, sampler T8 read 45 cfm and all the others were set as before in run 2. The cloud rose in a mushroom shape and extended to 150 to 200 ft. The cloud drifted at approximately 2 mph over the trees east of the target. The part of the cloud closest to the ground passed through the downwind sampler group. After the shot, the sampler flowmeters read as set initially except for T1-T6, I1, I2, which read below scale or zero. The Lundgren impactors were allowed to run during the preparations for the next firing.

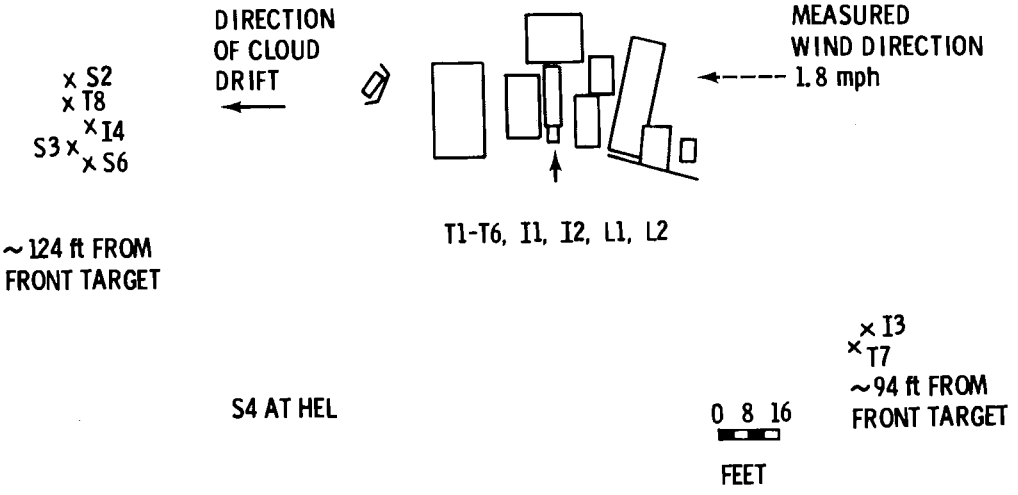

FIGURE A.1.3. Sampler Placement Run 3, October 6, 1977

TABLE A.1.3. Sampler Operation, Run 3, October 6, 1977

Sampler	Time on	Time off	Duration (min)	Assumed Average Flowrate, cfm
T1-T6	1716	1738	?	50
T7	1716	1738	22	50
T8	1716	1738	22	45
I1, I2	1716	1738	?	20
I3, I4	1716	1738	22	20
L1, L2	1716	1800	44	3
S2	1716	1738	22	26
S3	1716	1738	22	26
S6	1716	1738	22	35
S4	1515	1815	180	24

RUN 4--OCTOBER 7, 1977, ROUND 5 FIRED 1401 and 1508

The first round was fired at 1401 hr, and the cloud drifted at about 4 mph over samplers I3 and T7 (which were initially the upwind samplers). The authors intended to operate the Lundgren impactors and upwind/downwind samplers undisturbed for an hour with none of the usual activity in the target area. The air sampling crew entered the target area at 1416 hr to shut off some of the samplers and adjust the others. At this time, T8 read 48 cfm (it had initially read 43 cfm). Samplers T1-T6, I1, and I2 read below scale and were shut off. All the remaining samplers were operating at their initial flow rate.

The air sampling crew returned to the target area at 1440 hr and turned off the Lundgren impactors, which were still operating at 3 cfm. The upwind/downwind samplers were left on for the next round. The target area samplers were removed and the usual preparations for a shot commenced. The second round was fired at 1508 hr. The cloud drifted over samplers T7 and I3. The upwind/downwind samplers were turned off at 1536 hr.

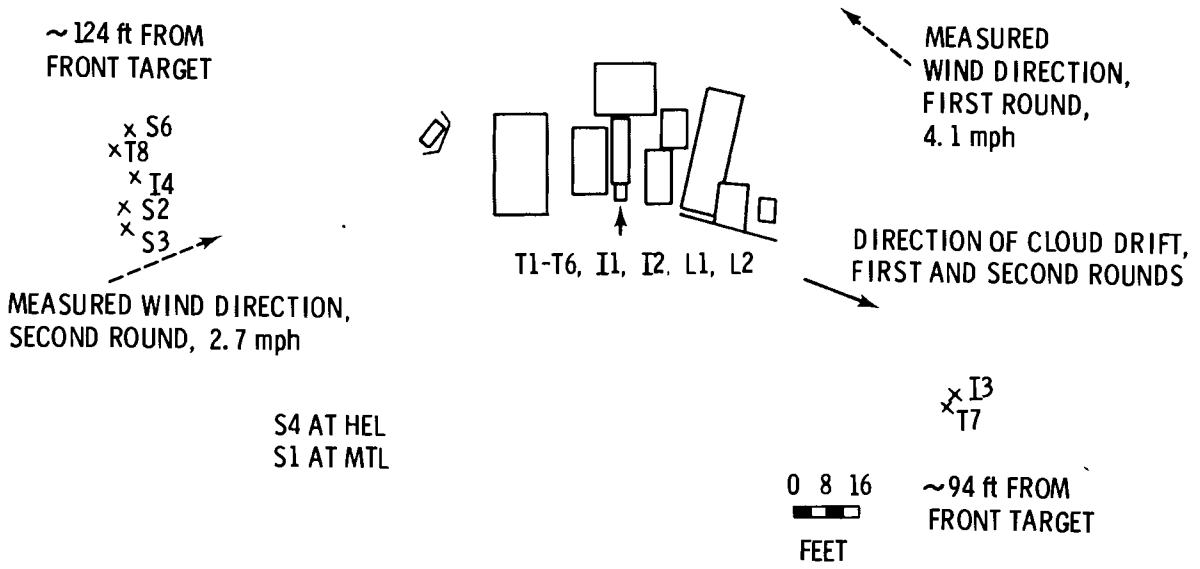

FIGURE A.1.4. Sampler Placement Run 4, October 7, 1977

TABLE A.1.4. Sampler Operation, Run 4, October 7, 1977

Sampler	Time on	Time off	Duration (min)	Assumed Average Flowrate, cfm
T1-T6	1352	1417	?	50
T7	1352	1535	103	50
T8	1352	1535	103	46
I1, I2	1352	1417	?	20
I3, I4	1352	1535	103	20
L1, L2	1352	1440	48	3
S2, S3	1352	1535	103	26
S6	1352	1535	103	35
S1	1458	1945	287	25
S4A	1251	1612	201	24
S4B	1655	1920	145	24

RUN 5--OCTOBER 8, 1977, ROUND FIRED 0850

The cloud drifted to the northwest of the target and over samplers T7 and I3. The back-up filter holder for impactor L1 was found disconnected from the impactor, possibly because of the concussion of the round, and was reconnected at 0908 hr; however, the samples from L1 may be of little value.

The flow rates of most upwind/downwind samplers remained as set. The flow rates of samplers T1-T6, I1, and I2 were essentially zero after the samplers became plugged with particulates. The flow rate of sampler L2 had crept up to 4 cfm and was adjusted back down to 3 cfm at 0914 hr. The flow rates of samplers T8 and I4 had decreased to 40 and 15 cfm, respectively, by the time they were turned off.

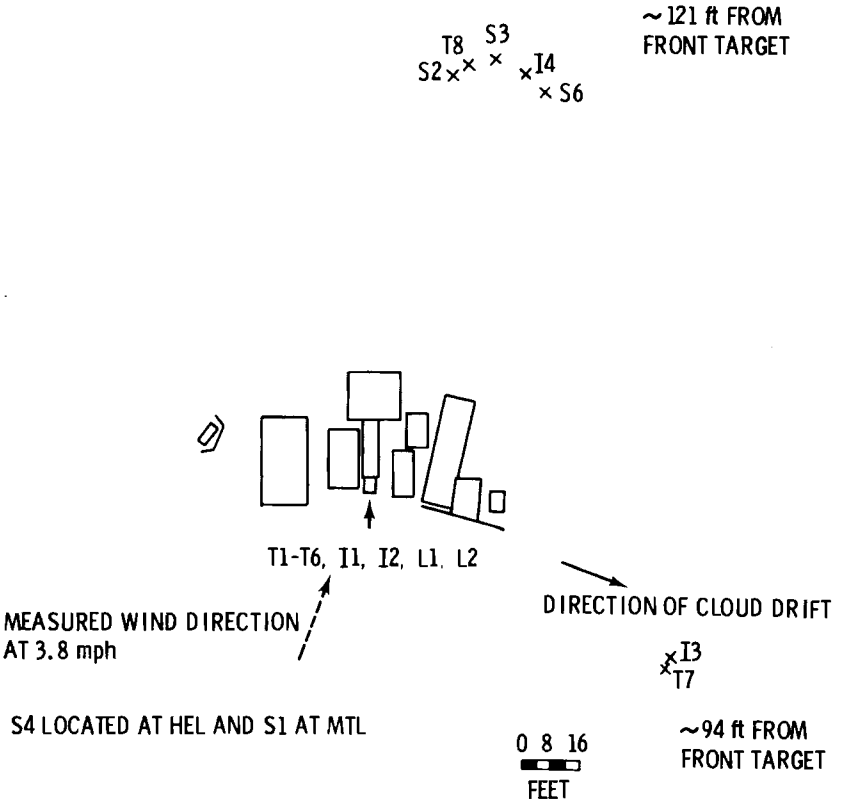

FIGURE A.1.5. Sampler Placement Run 5, October 8, 1977

TABLE A.1.5. Sampler Operation, Run 5, October 8, 1977

Sampler	Time on	Time off	Duration (min)	Assumed Average Flowrate, cfm
T1-T6	0843	0909	?	50
T7	0843	0909	26	50
T8	0843	0909	26	45
I1, I2	0843	0909	?	20
I3, I4	0843	0909	26	20
L1	0843	0930	?	3
L2	0843	0930	47	3
S2, S3	0843	0909	26	26
S6	0843	0909	26	35
S1	0650	1325	395	23
S4	0723	1232	309	24

APPENDIX A.2

METEOROLOGICAL DATA EXTRACTED FROM REPORT FURNISHED BY U.S. ARMY ENVIRONMENTAL HYGIENE AGENCY, AGP, MD, DATED NOVEMBER 15, 1977

TABLE A.2.1. AEHA Meteorological Data for Time Periods October 4, 1977 to October 9, 1977

Date	Time[a]	Wind Speed (mph)[b]	Wind Direction (°)	Sigma (°)	Stability Class
October 4, 1977					
Run 1, Round 1803	1800-1900	2.8	283		B2
		1.7	282		B2
		1.8	319		B2
		1.1	54		B2
		1.0	4		B2
		CALM			
		CALM			
		CALM			
		CALM			
		CALM			
		CALM			
		CALM			
October 6, 1977					
Run 2, Round 0951	0945-1040	2.3	114		
		1.5	6		
		1.0	322		
		2.5	291		
		1.8	206		
		2.1	294		B1
		1.0	293		B1
		1.8	226		B1
		1.3	315		B1
		1.3	276		B1
		CALM			

(a) Wind data reported at 5-min intervals.
(b) Calm is indicated when the wind speed dropped below 1 mph.

TABLE A.2.1. (Contd)

Date	Time[a]	Wind Speed (mph)[b]	Wind Direction (°)	Sigma (°)	Stability Class
October 6, 1977					
Run 3, Round 1722	1720-1820	1.8	274		B1
		1.5	359		B1
		1.3	100		B1
		CALM			B1
		CALM			B1
		1.2	258		B1
		1.3	193		B1
		1.3	206		B1
		2.1	280		B1
		1.7	218		B1
		1.3	295		B1
		CALM			B1
October 7, 1977					
Run 4, Round 4a, 1400	1401-1505	4.1	308		B1
		5.0	222		B1
		5.5	216		B1
		5.2	131		B1
		4.4	137		B1
		3.7	25		B1
		2.7	140		B2
		3.0	166		B2
		2.8	331		B2
		2.4	223		B2
		2.8	38		B2
		3.3	72		B2
		2.1	51		B2

TABLE A.2.1. (Contd)

Date	Time[a]	Wind Speed (mph)[b]	Wind Direction (°)	Sigma (°)	Stability Class
October 7, 1977					
Round 4b, 1508	1505-1600	2.7	61		B2
		3.0	56		B2
		4.6	120		B2
		8.0	133		B2
		7.3	129		B1
		8.4	100		B1
		3.8	351		B1
		4.8	155		B1
		7.0	144		B1
		4.5	308		B1
		5.7	218	24	B1
October 8, 1977					
Run 5, Round 0850	0845-0955	3.8	24	4	B1
		3.5	22	5	B1
		2.5	156	5	B1
		1.5	5	8	B1
		1.8	13	10	B1
		2.3	189	10	B1
		2.7	131	10	B1
		2.2	41	7	B1
		3.7	28	5	B2
		2.7	22	5	B2
		2.7	38	4	B2
		2.4	87	50	B2
		1.6	55	50	B2
		1.7	204	10	B2

(a) Wind data reported at 5-min intervals.
(b) Calm is indicated when the wind speed dropped below 1 mph.

APPENDIX B.1

PREPARATION OF SAMPLES FOR URANIUM ANALYSIS

The samples from the wet fallout, probe wash and Lundgren impactor back-up filter required no further preparation before being submitted for analysis by UST. The other samples were divided so that portions could be reserved for other types of analyses.

The dry fallout material was dried in an oven and weighed. The paper towels used to clean the trays on October 6 were also dried and weighed, and small fractions of both towels and fallout were weighed before they were submitted to UST.

The deposited samples on the 8-in. x 10-in. Whatman 41 filters from the total-particulate samplers and from the impactor back-up stages appeared uniform to the eye and to a beta radiation survey. The Whatman 41 filters were cut into sixteenths as shown in Figure B.1. (Two exceptions to this division will be discussed later.) Four of these sections were selected as samples from different quarters of the filter (see Figure B.1). These four selected pieces totaled one-fourth of the original sample and were further

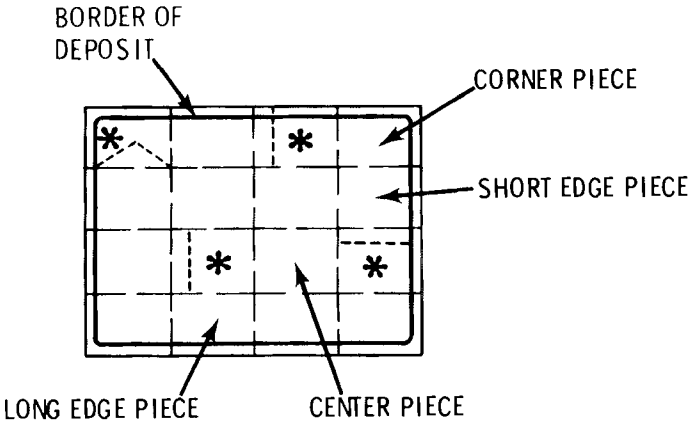

FIGURE B.1. Partitioning of 8-in. x 10-in. Filter

subdivided by removing one-fourth from each piece. A quarter from each selected one-fourth piece was submitted for analysis and the remaining parts reserved as spare samples; however, the spare samples were analyzed instead, ending in 3/16th of the original filter analyzed.

Two of the 8-in. x 10-in. total-particulate samples were brushed and scraped to attempt to remove most of the radioactive material from the filter surface. This material was to be analyzed for uranium oxide forms by X-ray diffraction. However, since no significant amount of radioactive material was removed, the two filters were cut and prepared for analysis as described above.

The 12-in.-dia, perforated, high-volume impactor substrates were cut into quarters radially. Two quarters from opposite sides of the substrate were then cut in half, and half from each quarter was submitted to UST, as shown in Figure B.2.

The authors intended originally to analyze each entire 12-in. substrate and respective swabs together as one sample; however, sectioning the substrates required that the swabs (approximately 100) be divided or analyzed separately. However, the swabs could not be accurately divided into equal

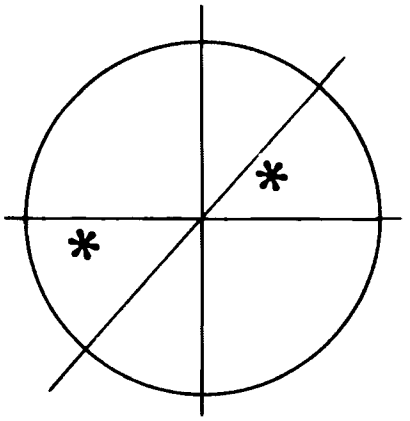

FIGURE B.2. Division of High-Volume Impactor 12-in. Substrates (the asterisk indicates portions sent to UST)

parts because the authors felt the uranium content would not be uniformly distributed. Therefore, swabs from four impactors were submitted for analysis -- two each from the target area impactors and the upwind/downwind impactors. From the results, average ratio (swab/substrate) uranium contents were calculated for each stage. The swabs were later dropped from the data because their inclusion had an insignificant effect on the resulting size distributions.

The 4-in. dia. Whatman 41 filters from the Staplex samplers were quartered radially. The opposite quarters were submitted for analysis by UST, as shown in Figure B.3.

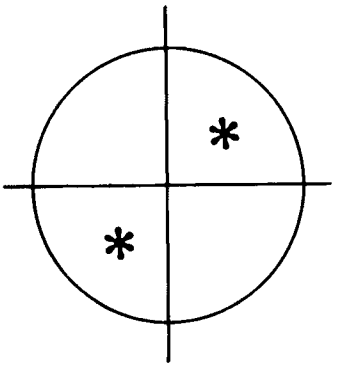

FIGURE B.3. Division of Staplex 4-in. Filter Samples (asterisk indicates portions submitted for analysis)

APPENDIX B.2

PREPARATION OF LUNDGREN IMPACTOR SUBSTRATES FOR ANALYSIS

The drums around which the mylar substrates were fastened during operation of the Lundgren impactor had a circumference of 4.5 in. (excluding a substrate hold-down). The mylar substrate deposit area was 1.9-in. wide, making the total particulate deposit area 1.9 x 4.5 in. As shown in Figure 18, time proceeds from right to left on the substrate. The substrates in Figure 18 show particularly high particle concentrations when the penetrator was fired and later during installation of new targets. (Only in Run 3 were there visibly distinct bands much later after the firing.)

Each substrate was cut into as many as 8 time increments. Generally, all the substrates from one impactor were cut into the same number of pieces. Ideally, the division into time increments should be identical for each substrate of an impactor; however, there was some variation because none of the visible bands (deposits) were cut and some of the bands ran together. The error, thus, introduced into the final concentration for each time interval calculation was small because the differences between the uranium content of the visible bands and of the other areas were large.

Figure 18 shows the segments into which the substrates from Run 3-L1 were cut. The impactors from Runs 1, 2, 3, and 5 were operated during the test firing and during the normal routine of replacing the targets. The substrates from these runs were cut into 5 to 6 bands. The Lundgren impactors from Run 4 were operated for about one hour after the test firing when there was no activity in the target area except the shutting off of other samplers. The Lundgren substrates from Run 4 were cut into 8 bands each. The widths of all bands were recorded so that the measured uranium content could be related to an approximate time interval.

Each piece of substrate was placed in a labelled 35-mm slide holder and backed with a larger piece of clean mylar. The slide frame mounts were used to enable the automatic and unattended changing of samples in the X-ray fluorometer. The samples were submitted to PNL's Chemical Methods and Kinetics Section for X-ray fluorescence analysis.

APPENDIX B.3

SAMPLE DATA REDUCTION FOR A LUNDGREN IMPACTOR, RUN 3-L1

TABLE B.3.1. Sample Data Reduction for a Lundgren Impactor, Run 3-L1

Substrate	Variable[a]	Segment Group[b] A	B	C and D	E	F	Total Mass Uranium µg	
S1	W	0.611	0.949	0.907	0.993	1.068		
	T	7.8	12.0	11.5	12.6	13.6		
	F	0.92	0.99	0.99	1.0	1.0		
	X	484.0	3.09	27.4	9.41	7.51		
	g	4000.0	37.0	310.0	120.0	99.0	4,600	
S2	W	0.219	1.346	0.749	1.104	1.037		
	T	2.8	17.1	9.5	14.0	13.2		
	F	0.42	1.0	0.96	1.0	1.0		
	X	278.0	4.07	4.87	2.01	4.89		
	g	1800.0	68.0	47.0	27.0	62.0	2,000	
S3	W	0.290	1.266	0.718	1.188	1.066		
	T	3.7	16.1	9.1	15.1	13.5		
	F	0.53	1.0	0.95	1.0	1.0		
	X	159.0	0.618	1.27	0.345	2.08		
	g	1100.0	9.6	12.0	5.1	27.0	1,200	
S4	W	0.355	1.139	0.780	1.149	1.079		
	T	4.5	14.5	9.9	14.6	13.7		
	F	0.63	1.0	0.97	1.0	1.0		
	X	207.0	2.16	2.51	3.25	1.99		
	g	1400.0	30.0	25.0	46.0	26.0	1,500	
Subtotal Mass, µg		8300.0	145.0	390.0	200.0	214.0	9,200	
% of Total[c]		90.2	1.6	4.2	2.2	2.3		
Analysis of back-up filter = 1470 µg								
Distributed Amount of Back-up Filter Uranium, µg		1300.0	24.0	62.0	30.0	34.0	1,400	
Total Mass Uranium			9600.0	170.0	450.0	230.0	250.0	10,700

(a) Where:

W = Segment width, in.
T = Time, min = 0.0788 W
F = Calibration factor
X = Analysis, $\mu g/cm^2$

$\mu g = 12.3 \frac{XW}{F}$ micrograms

(b) The segment group was comprised of the four segments (one from each substrate) corresponding to a time interval denoted by a letter, e.g., "Segment Group F". See Figure 18 and page 31.

(c) The percentage of the total collected during each time increment was used to distribute the uranium on the back-up filter among the time increments.

APPENDIX B.4

PREPARATION OF SAMPLES FOR OXIDE ANALYSIS

The analyses of target-area total-particulate and dry fallout samples were performed by the Metallurgy Research Section, PNL. The target-area total-particulate samples had already been cut as shown in Figure B.1. A single center piece of one sample from each run was submitted for analysis. The samples selected were:

Run 1-T2
Run 2-T1
Run 3-T2
Run 4-T3
Run 5-T2

Small fractions of the dry fallout samples were also submitted for analysis.

The analysis of two sets of high-volume cascade impactor substrates were performed by the Analytical and Nuclear Research Section, PNL. Fractions of the four substrates and back-up filter were submitted from each of the impactors Run 3-I2 and Run 4-I2. These samples were already divided as shown in Figures B.1 and B.2. A short edge piece from each of the back-up filters was analyzed. One-eighth of the substrates from Run 3-I2 and one-sixteenth from Run 4-I2 were analyzed. Pieces of Whatman 41 media were submitted to both sections as blanks.

APPENDIX B.5

METHODS FOR OXIDE ANALYSIS

The X-ray diffraction of the total-particulate and fallout samples was obtained by diffractometer tracing 2θ angles (angle between incident and diffracted beam) from 10° to 70° on a fraction of each sample. The crystalline phase was identified by comparing the intensity and the 2θ angles of the diffraction peaks with those of 24 uranium oxides listed in the American Society for Testing Materials Diffraction File. A semiquantitative estimate of the relative abundance of the uranium oxides present was determined by comparing the integrated diffraction intensities (peak areas) from the two phases. The uncertainty of this comparison is estimated at 15%.

The size and morphology of the fallout particles and target-area total-particulate samples were examined using an SEM. The elemental composition of the particles was analyzed using an X-ray fluorescence microprobe. The microprobe could not analyze for the oxides, however.

The high-volume cascade impactor samples were analyzed using techniques similar to those described above: X-ray diffractometer, SEM and X-ray fluorescence microprobe. Uranium oxides were identified but not quantified.

APPENDIX B.6

SAMPLE PREPARATION FOR SOLUBILITY MEASUREMENTS

The solubility of uranium-containing particles was investigated using simulated lung fluids. Samples of target-area total particulates and respirable particles from the target area and downwind were used for this measurement.

Fractions of the high-volume cascade impactor samples Run 3-I2, Run 4-I2 (target area), and Run 4-I3 (downwind) were prepared for solubility analysis. The particles smaller than 3.3-μm AED were assumed to be respirable; therefore, one-eighth of substrates Numbers 3 and 4 and the back-up filter were analyzed. These samples were sectioned as shown in Figures B.1 and B.2. (A corner piece and a center piece of the 8- x 10-in. back-up filter contain approximately one-eighth of the deposited particulates.) The fractions were combined so that there was one composite sample for each impactor.

A center piece from each of the target-area total-particulate samples listed in Appendix B.4 was analyzed. Each piece contained approximately 8.2% of the deposited particulates on the filter.

In total, three composite impactor samples and five total-particulate samples were submitted for analysis. Blanks of Whatman 41 media were also analyzed.

APPENDIX B.7

METHOD FOR SOLUBILITY ANALYSIS

The solubilities of the materials collected were measured by immersing the samples in simulated lung fluid and extracting aliquots at pre-selected times. (PNL's Inhalation Technology and Toxicology Section performed the analysis.) The filter paper sections were immersed in bottles containing 55 ml of fluid held at 37°C, and gas (5% CO_2 in O_2 to prevent a pH shift of the solution) was bubbled through the fluid until the free volume of the containers was swept free of air. The bottles were capped and placed in a shaker bath maintained at 37°C (body temperature). The initial pH of the fluid was 7.4. Three sets of duplicate samples were taken: one immediately after wetting, one after one week, and one after four weeks. Samples were extracted by injecting a volume of gas into the bottle and then removing an equivalent volume of solution containing a representative quantity of filter paper and solids. (Removing an equivalent quantity of all materials during each extraction means the solution remaining is always representative of the initial volume.) Each volume extracted (duplicate 1-ml aliquots) was forced through a membrane filter (0.1-μm mean pore size), and the uranium content was measured by fluorometry (at UST, Richland Division).

APPENDIX C

SAMPLE SIZE DISTRIBUTION DATA REDUCTIONS

TABLE C.1. High-Volume Cascade Impactor Example Size Distribution Run 1-I1

Stage	Aerodynamic Cut Off Dia., μm	Uranium on Sample, μg	% per Stage	Cumulative %
Probe		3.85×10^4		
1	7.0	1.48×10^4	38.2	100.1
2	3.3	1.11×10^4	8.0	61.8
3	2.0	0.596×10^4	4.3	53.9
4	1.1	0.281×10^4	2.0	49.6
Filter		6.64×10^4	47.6	47.6
		1.40×10^5		

TABLE C.2. Size Distribution Calculations for Lundgren Impactor Run 3-L1

Stage	Equivalent Cut Off Diameter, μm	Segment Group A[a] Uranium, μg	%	Cumulative %	All Segment Groups[b] Uranium, μg	%	Cumulative %
1	9.4	4,000	41.7	100.1	4,600	43.0	100.0
2	2.8	1,800	18.8	58.4	2,000	18.7	57.0
3	0.9	1,100	11.5	39.6	1,200	11.2	38.3
4	0.26	1,400	14.6	28.1	1,500	14.0	27.1
Back-up Filter		1,300	13.5	13.5	1,400	13.1	13.1
Total		9,600			10,700		

(a) See page B5. These samples include material collected at the instant of the test firing.
(b) These samples include material collected during the entire operating time of the sampler.

APPENDIX D

AIRBORNE URANIUM CONCENTRATION IN TARGET AREA VERSUS TIME

TABLE D.1. Sample Calculations of Average Concentration per Time Interval

Sampler	Time After Shot, min.	Item	Segment Group[a] A	B	C	D	E	F
Run 4-L1	39	Ave Time, min	6.1	6.4	6.3	6.3	6.2	6.3
		Σ Time	6.1	12.5	18.8	25.1	31.3	37.6
		μg collected	18,100.0	208.0	136.0	74.0	51.0	61.0
		$\mu g/m^3$	3.5×10^4	3.8×10^2	2.5×10^2	1.4×10^2	9.7×10^1	1.1×10^2
Run 4-L2	39	Ave Time	4.1	6.4	6.6	6.5	6.3	6.2
		Σ Time	4.1	10.5	17.1	23.6	29.9	36.1
		μg	2,780.0	18.7	10.1	6.1	3.4	2.5
		$\mu g/m^3$	8.0×10^3	3.4×10^1	1.8×10^1	1.1×10^1	6.4×10^0	4.7×10^0

Concentration $\mu g/m^3 = \mu g \cdot \frac{min}{3\ ft^3} \cdot \frac{1}{T,\ min} \cdot \frac{35.31\ ft^3}{m^3}$ where the samplerflow was 3 cfm

(a) Represents sample collected during time interval A, B, etc. See page B.5.

TABLE D.2. Average Concentration per Time Interval

Impactor	Time Interval, min	Interval Midpoint, min	Average Uranium Concentration $\mu g/m^3$
Run 1-L2[a]	0-5.8	2.9	28,000
	5.8-21.8	13.8	170
	21.8-37.8	29.8	29
	37.8-49.0	43.4	100
Run 2-L2	0-4.1	2.1	18,000
	4.1-18.1	11.1	120
Run 3-L2	0-5.4	2.7	18,000
	5.4-19.4	12.4	53
	19.4-33.4	26.4	34
	33.4-38.0	35.7	170
Run 4-L2	0-4.1	2.1	8,000
	4.1-10.5	7.3	34
	10.5-17.1	13.8	18
	17.1-23.6	20.4	11
	23.6-29.9	26.8	6.4
	29.9-36.1	33.0	4.7
Run 5-L2	0-4.3	2.2	18,000
	4.3-18.2	11.3	70
	18.2-32.8	25.5	45
	32.8-40.0	36.4	31
Run 1-L1[b]	0-9.0	4.5	21,000
	9.0-13.6	11.3	1,800
	13.6-32.5	23.1	110
	32.5-49.0	40.8	170
Run 3-L1	0-4.7	2.4	24,000
	4.7-19.7	12.2	130
	19.7-29.7	24.7	530
Run 4-L1	0-6.1	3.1	35,000
	6.1-12.5	9.3	380
	12.5-18.8	15.7	250
	18.8-25.1	22.0	140
	25.1-31.3	28.2	97
	31.3-37.6	34.5	110

(a) L2 - Sampler Behind Film Frame
(b) L1 - Target Accessway Sampler

APPENDIX E

CONCENTRATION OF TOTAL EXPOSURE IN TARGET AREA

TABLE E.1. Calculation of Total Exposure in Target Area[a]

Sampler	Uranium Collected, mg	Exposure, mg min/m^3
Run 1 - T1	252	178
T2	264	186
T3	164	116
T4	207	146
T5	218	154
T6	172	121
Total	1277	150
Run 2 - T1	305	215
T2	152	107
T3	172	121
T4	166	117
T5	79.1	55.9
T6	422	298
Total	1296	153
Run 3 - T1	492	347
T2	387	273
T3	280	198
T4	262	185
T5	238	168
T6	169	119
Total	1828	215
Run 4 - T1	316	223
T2	271	191
T3	483	341
T4	299	211
T5	283	200
T6	313	221
Total	1965	231
Run 5 - T1	308	218
T2	329	232
T3	270	191
T4	178	126
T5	195	138
T6	194	137
Total	1474	173

(a)Exposure = mg/(50 cfm x .02832)
Total Exposure = Total mg/(300 cfm x .02832)
where: cubic foot = .02832 m^3
See page 44

DISTRIBUTION

No. of Copies

OFFSITE

A. A. Churm
DOE Chicago Patent Group
9800 South Cass Avenue
Argonne, IL 60439

Office of Secretary of Defense
(Health Affairs)
ATTN: LTC B. Chase
Pentagon, Room E171
Washington, DC 20301

Office of Secretary of Defense
Office of Director of Defense
Research and Engineering
ATTN: Mr. J. Persh
Washington, DC 20301

Office of Assistant Secretary
of Defense for Atomic Energy
ATTN: Cmdr. G. Cliff
Pentagon, Room 3E1069
Washington, DC 20301

Honorable Percy A. Pierre
Assistant Secretary of the Army
for Research, Development and
Acquisition
Department of the Army
Washington, DC 20310

Office of the Undersecretary
of the Army
Deputy Undersecretary
(Operations Research)
ATTN: Mr. D. Hardison
Department of the Army
Washington, DC 20310

No. of Copies

Undersecretary of Defense for
Research and Engineering
Deputy Undersecretary
(Tactical Warfare Programs)
Department of Defense
Washington, DC 20310

Undersecretary of Defense for
Research and Engineering
Deputy Undersecretary
(Tactical Warfare Programs)
ATTN: Mr. C. McKinley
Department of Defense
Washington, DC 20310

Undersecretary of Defense for
Research and Engineering
Deputy Undersecretary
(Tactical Warfare Programs)
ATTN: Mr. R. Moore
Department of Defense
Washington, DC 20310

Undersecretary of Defense for
Research and Engineering
Deputy Undersecretary (Research
and Advanced Technology)
ATTN: Dr. Ruth Davis
Department of Defense
Washington, DC 20310

Office of the Deputy
Undersecretary of Defense,
Research and Engineering
ATTN: Mr. R. Thorkildsen
Pentagon
Washington, DC 20301

Headquarters
Department of the Army
ATTN: DASG-TSP-E, COL Wangemann
Washington, DC 20310

No. of Copies

Commander
U.S. Army Combined Arms Combat Development Activity
ATTN: APCA-BC
Fort Leavenworth, KS 66027

Commander
U.S. Army Environmental Hygiene Agency
ATTN: HSE-O, COL J. Thiessen
Aberdeen Proving Ground, MD 21005

20 Commander
U.S. Army Armament Research and Development Command
ATTN: DRDAR-SCM-P, Dr. E. Bloore
Dover, NJ 07801

Director
U.S. Army Human Engineering Laboratory
ATTN: DRXHE-HE, Mr. Erickson
Aberdeen Proving Ground, MD 21005

Headquarters
Department of the Army
ATTN: DACS-DMT
Washington, DC 20310

Headquarters
Department of the Army
ATTN: DAMA-ARX-A, Dr. M. Lasser
Washington, DC 20310

Headquarters
Department of the Army
ATTN: DAMA-CSS, Dr. J. Bryant
Washington, DC 20310

Headquarters
Department of the Army
ATTN: DAMA-CSM, LTC German
Washington, DC 20310

No. of Copies

Headquarters
Department of the Army
ATTN: DAMA-CSM-CA, Mr. Lippi
Washington, DC 20310

Headquarters
Department of the Army
ATTN: DAMA-WSW, LTC Hinson
Washington, DC 20310

Headquarters
Department of the Army
ATTN: DAMA-WSZ-A
Washington, DC 20310

Project Manager
XM1 Tank System
ATTN: DRCPM-GCM BG Babers
Warren, MI 48092

Project Manager
XM1 Tank System
ATTN: DRCPM-GCM-SI, Mr. D. Bartle
Warren, MI 48090

Project Manager
Tank Main Armament System
ATTN: DRCPM-TMA-120mm, COL Appling
Dover, NJ 07801

Project Manager
Tank Main Armament System
ATTN: DRCPM-TMA, MAJ Michlik
Dover, NJ 07801

Project Manager
Division Air Defense Gun
ATTN: DRCPM-ADG
Dover, NJ 07801

Project Manager
Production Base Modernization and Exp
ATTN: DRCPM-PBM, Mr. C. Kolis
Dover, NJ 07801

No. of
Copies

Project Manager
M60 Tank
Michigan Army Missile Plant
ATTN: DRCPM-M60
Warren, MI 48090

Commander
U.S. Army Logistics Center
ATTN: ATCL-M, Mr. Thompson
Fort Lee, VA 23801

Commander
U.S. Army Missile Munitions
ATTN: ATSK-CD
Redstone Arsenal, AL 35809

Commander
U.S. Army Logistics Evaluation
Agency
ATTN: DALO-LEI, Mr. Frye
New Cumberland Army Depot
New Cumberland, PA 17070

Commander
U.S. Army Materiel Development
and Readiness Command
ATTN: DRCDR-DW, COL Collins
5001 Eisenhower Avenue
Alexandria, VA 22333

Commander
U.S. Army Materiel Development
and Readiness Command
ATTN: DRCQA, Mr. R. Fahy
5001 Eisenhower Avenue
Alexandria, VA 22333

Commander
U.S. Army Materiel Development
and Readiness Command
ATTN: DRCDMD, LTG R. J. Baer
5001 Eisenhower Avenue
ALexandria, VA 22333

No. of
Copies

Commander
U.S. Army Materiel Development
and Readiness Command
ATTN: DRCBSI, MG I. Hunt
5001 Eisenhower Avenue
Alexandria, VA 22333

Commander
U.S. Army Materiel Development
and Readiness Command
ATTN: DRCDMA-ST
5001 Eisenhower Avenue
Alexandria, VA 22333

Commander
U.S. Army Materiel Development
and Readiness Command
ATTN: DRCSMA-ST, COL Vincent
5001 Eisenhower Avenue
Alexandria, VA 22333

Commander
U.S. Army Materiel Development
and Readiness Command
ATTN: DRCSG, COL R. Cutting
5001 Eisenhower Avenue
Alexandria, VA 22333

Commander
U.S. Army Materiel Development
and Readiness Command
ATTN: DRCPA-E, Mr. Pace
5001 Eisenhower Avenue
Alexandria, VA 22333

Commander
U.S. Army Materiel Development
and Readiness Command
ATTN: DRCSF-P, Mr. Taras
5001 Eisenhower Avenue
Alexandria, VA 22333

Director
DARCOM Field Safety Activity
ATTN: DRXOS-ES, Mr. E. Olsen
Charlestown, IN 47111

No. of Copies

Director
U.S. Army Materials and
Mechanics Research Center
ATTN: DRXMR-X, Dr. E. Wright
Watertown, MA 02172

Director
U.S. Army Materials and
Mechanics Research Center
ATTN: DRXMR-AR, Mr. S. Levin
Watertown, MA 02172

Director
U.S. Army Materiels Systems
Analysis Agency
ATTN: DRXSY
Aberdeen Proving Ground, MD 21005

Director
U.S. Army Materiels Systems
Analysis Agency
ATTN: DRXSY-GA, Mr. W. Brooks
Aberdeen Proving Ground, MD 21005

Director
U.S. Army Materiels Systems
Analysis Agency
ATTN: DRXSY-GA, Mr. J. McCarthy
Aberdeen Proving Ground, MD 21005

Director
U.S. Army Materiels Systems
Analysis Agency
ATTN: DRXSY-GA, Mr. R. Smith
Aberdeen Proving Ground, MD 21005

Commander
U.S. Army Armament Materiel
Readiness Cmd
ATTN: DRSAR-MAD-C, Mr. P. Shaw
Dover, NJ 07801

Commander
U.S. Army Armament Materiel
Readiness Cmd
ATTN: DRSAR-ASR, LTC Counihan
Rock Island, IL 61201

No. of Copies

Commander
U.S. Army Armament Research
and Development Cmd
ATTN: DRDAR-CG, MG A. Light
Dover, NJ 07801

Commander
U.S. Army Armament Research
and Development Cmd
ATTN: DRDAR-TD, Dr. R. Weigle
Dover, NJ 07801

Commander
U.S. Army Armament Research
and Development Cmd
ATTN: DRDAR-SC, Dr. D. Gyorog
Dover, NJ 07801

Commander
U.S. Army Armament Research
and Development Cmd
ATTN: DRDAR-LC, Dr. J. Frasier
Dover, NJ 07801

Commander
U.S. Army Armament Research
and Development Cmd
ATTN: DRDAR-LC, Dr. J. Frasier
Dover, NJ 07801

Commander
U.S. Army Armament Research
and Development Cmd
ATTN: DRDAR-SCM, J. Corrie
Dover, NJ 07801

Commander
U.S. Army Armament Research
and Development Cmd
ATTN: DRDAR-LCU-D-T, Mr. Davitt
Dover, NJ 07801

No. of Copies

Commander
U.S. Army Armament Research & Development Cmd
ATTN: DRDAR-SF, Mr. Elliott
Dover, NJ 07801

Commander
U.S. Army Armament Research & Development Cmd
ATTN: DRDAR-BLT, Mr. R. Vitali
Aberdeen Proving Ground, MD 21005

Commander
U.S. Army Armament Research and Development Cmd
ATTN: DRDAR-BLT, Dr. W. Gillich
Aberdeen Proving Ground, MD 21005

Commander
U.S. Army Armament Research and Development Cmd
ATTN: DRDAR-BLV, Mr. E. Wilsey
Aberdeen Proving Ground, MD 21005

Commander
U.S. Army Armament Research and Development Cmd
ATTN: DRDAR-BLP, Mr. R. Comer
Aberdeen Proving Ground, MD 21005

Commander
U.S. Army Armament Research and Development Cmd
ATTN: DRDAR-AD-SA, Mr. Markland
Aberdeen Proving Ground, MD 21005

Commander
U.S. Army Armament Research and Development Cmd
ATTN: DRDAR-LCB, Mr. P. Rummel
Watervliet, NY 12189

Director
U.S. Army Ammunition Center
ATTN: SARAC-D, Mr. K. Croscost
Savanna, IL 61074

No. of Copies

Commander
U.S. Army Armament Materiel Readiness Cmd
ATTN: DRSAR-CG
Rock Island, IL 61201

Commander
U.S. Army Armament Materiel Readiness Cmd
ATTN: DRSAR-LEA, Mr. E. Beckman
Rock Island, IL 61201

Commander
U.S. Army Armor Center and School
ATTN: MG T. V. Lynch
Fort Knox, KY 40121

Commander
U.S. Army Armor Center and School
ATTN: Mr. M. Falkovitch
Fort Knox, KY 40121

Commander
U.S. Army Missile Command
ATTN: DRCPM-LCE, Mr. Crosswhite
Redstone Arsenal, AL 35809

Commander
U.S. Army Mobility Equipment Research and Development Cmd
ATTN: DRSME-RZT, Tech Doc Ctr B/315
Fort Belvoir, VA 22060

Commander
U.S. Army Research Office
ATTN: Dr. G. Mayer
P. O. Box 12211
Research Triangle Park, NC 27709

Commander
U.S. Army Research Office
ATTN: Dr. E. Saibel
P. O. Box 12211
Research Triangle Park, NC 27709

No. of Copies

Commander
U.S. Army Tank Automotive
Research and Development Cmd
ATTN: DRDTA-RWL
Warren, MI 48090

Commander
U.S. Army Tank Automotive
Research and Development Cmd
ATTN: DRDTA-RKA, Mr. V. Pagano
Warren, MI 48090

Commander
U.S. Army Test & Evaluation Cmd
ATTN: DRSTE
Aberdeen Proving Ground, MD 21005

Commander
U.S. Army Test & Evaluation Cmd
ATTN: DRSTE-AR, Mr. Brown
Aberdeen Proving Ground, MD 21005

Commander
U.S. Army Test & Evaluation Cmd
ATTN: DRSTE-CE
Aberdeen Proving Ground, MD 21005

Commander
U.S. Army Test & Evaluation Cmd
ATTN: DRSTE-PP-E
Aberdeen Proving Ground, MD 21005

Commander
U.S. Army Test and Evaluation Cmd
ATTN: DRSTE-ST, Mr. J. Starkey
Aberdeen Proving Ground, MD 21005

Commander
U.S. Army Training and
Doctrine Cmd
Fort Monroe, Hampton, VA 23651

No. of Copies

Director
U.S. Army TRADOC Systems
Analysis Act
ATTN: ATAA-SA
White Sands Missile Range, NM 88002

Commander
U.S. Army Foreign Science &
Technology Center
ATTN: DRXST-CB, J. Bollendorf
Building 220
7th Street, NE
Charlottesville, VA 22901

Commander
Naval Facilities Engineering Cmd
Code 04N2, Mr. G. Hendrix
200 Stovall Street
Alexandria, VA 22333

Commander
U.S. Naval Ordinance Systems Cmd
ATTN: ORD-9132
Washington, DC 20360

Superintendent
U.S. Naval Postgraduate School
ATTN: Dir. of Lib.
Monterey, CA 93940

Commander
Naval Sea Systems Cmd
ATTN: PMS-404-31,
Mr. E. Gerlach
Washington, DC 20362

Commander
U.S. Naval Surface Weapons
Center
ATTN: Code WR-32,
Dr. S. Fishman
White Oak, MD 20910

No. of Copies

Commander
U.S. Naval Surface Weapons Center
ATTN: Code DG-52, W. Wishard
White Oak, MD 20910

Commander
U.S. Marine Corps Liaison Office
Aberdeen Proving Ground, MD 21005

Commander
U.S. Air Force Headquarters
ATTN: SG-PA, LTC J. Bayer
Washington, DC 20314

HQ, CMS/EE
ATTN: TSGT Cirilo
Nellis AF Base, NV 89191

HQ, ADTC/SCV
ATTN: MAJ R. Conrad
Eglin AFB, FL 32542

HQ ADTC/DLV
ATTN: Dr. J. Cornette
Englin AFB, FL 32542

Commander
U.S. Air Force Tactical Air Cmd
ATTN: SG-PA, LTC J. Couglin
Langley AFB, VA 23665

National Lead Company of Ohio
ATTN: Mr. L. Levy
Box 39158
Cincinnati, OH 45239

Rockwell International
Rocky Flats Plant
ATTN: Dr. M. Werkema
Bldg. 123, P. O. Box 464
Golden, CO 80401

No. of Copies

The Analytic Sciences Corporation
ATTN: Dr. S. Bucci
6 Jacob Way
Reading, MA 01867

Union Carbide Corporation
Nuclear Division
ATTN: Mr. M. Sanders
P. O. Box Y
Oak Ridge, TN 37830

Nuclear Regulatory Commission
Division of Fuel Cycle and Material Safety
ATTN: Mr. E. Wright
Washington, DC 20555

University of California
Los Alamos Scientific Laboratory
ATTN: Dr. D. Sandstrom, CMB-6
Los Alamos, NM 87544

Air Force Materiel Laboratory
ATTN: LTM S. Inouye
Wright-Patterson AFB, OH 45433

Air Force Materiel Laboratory
ATTN: YXD, CPT D. Schuur
Wright-Patterson AFB, OH 45433

HQ, ADTC
ATTN: CEEDO/CC Detachment 1
Tyndall AFB, FL 32403

USA Ordnance Center and School
Aberdeen Proving Ground, MD 21005

Headquarters
Department of the Army
ATTN: DAMO-RQD, LTC Idey
Washington, DC 20310

No. of
Copies

Headquarters
Department of the Army
ATTN: DAMO-TRS, LTC Lyon
Washington, DC 20310

Headquarters
Department of the Army
ATTN: DAMO-TRI, MAJ Steedy
Washington, DC 20310

Headquarters
Department of the Army
ATTN: DAIG-SD, Mr. J. Coakley
Washington, DC 20310

Headquarters
Department of the Army
ATTN: DALO-TSP, LTC Deakey
Washington, DC 20310

Headquarters
Department of the Army
ATTN: DALO-SMS, Ms. T. Ueckert
Washington, DC 20310

Headquarters
Department of the Army
ATTN: DASC-DPA, LTC Rogers
Washington, DC 20310

Headquarters
Department of the Army
ATTN: DAEN-ZCE, COL Herndon
Washington, DC 20310

Headquarters
Department of the Army
ATTN: SARDA, COL Drudvig
Washington, DC 20310

Headquarters
Department of the Army
ATTN: SAIL-SN, Mr. Hildebrand
Washington, DC 20310

No. of
Copies

Headquarters
Department of the Army
ATTN: SAGC, Mr. Henke
Washington, DC 20310

Commander
U.S. Army Materiel Development
& Readiness Command
ATTN: DRCSG-R, LTC Bell
5001 Eisenhower Avenue
Alexandria, VA 22333

3 Commander
U.S. Army Armament Materiel
Readiness Cmd
ATTN: ERSAR-SS, Mr. B. Morris
Rock Island, IL 61201

Commander
U.S. Army Training and
Doctrine Cmd
ATTN: ATEM-SE, Mr. Dery
Fort Monroe, VA 23651

Commander
U.S. Army Training and
Doctrine Cmd
ATTN: ATTR-HR-S, Mr. Teichmann
Fort Monroe, VA 23651

Commander
U.S. Army Center and School
ATTN: ATZK-CG-AM-L,
LTC Robinson
Fort Knox, KY 40121

27 DOE Technical Information Center

ONSITE

DOE Richland Operations Office

H. E. Ransom

No. of
Copies

29 Pacific Northwest Laboratory

W. T. Bartlett
C. E. Elderkin
R. L. Gilchrist (3)
J. A. Glissmeyer (3)
R. K. Hadlock
M. A. Halvorsen
H. Larson
G. B. Long (2)
J. Mishima (2)
O. R. Moss
P. W. Nickola
G. B. Parker
L. C. Schwendiman
J. M. Selby
C. Unruh
R. K. Woodruff
Technical Information (5)
Publishing Coordination (2)